



**TRIBHUWAN UNIVERSITY  
INSTITUTE OF ENGINEERING  
PULCHOWK CAMPUS  
DEPARTMENT OF CIVIL ENGINEERING  
M.Sc. Program in Structural Engineering**

**Thesis No:-SS00129**

**EARTHQUAKE GROUND MOTION PARAMETERS  
FOR STRUCTURAL DESIGN IN NEPAL**

**Shailendra Kumar Sah**

**April 2009**



## COPYRIGHT ©

The author has agreed that the library, Department of Civil Engineering, Institute of Engineering, Pulchowk Campus, may this thesis freely available for inspection. Moreover, the author has agreed that the permission for extensive copying of this thesis for scholarly purpose may be granted by the Professor, who supervised the thesis work recorded or, in his absence, by Head of Department or concerning M.Sc. Program coordinator or Dean of the Institute in which thesis work was done. It is understood that the recognition will be given to the author of this thesis and to the Department of Civil Engineering, Pulchowk in any use of the material of thesis. Copying or publication or other use of the material of this for financial gain without approval of Department of Civil Engineering, Institute of Engineering, Pulchowk Campus and author's written permission is prohibited.

Request for permission to copy or to make any use of the material in this in whole or part should be addressed to:

.....  
Head of Department of Civil Engineering  
Institute of Engineering,  
Pulchowk Campus,  
Lalitpur, Nepal

## CERTIFICATE

*This is certified that the work contained in this thesis entitled “Earthquake Ground motion parameter for structural design in Nepal” being submitted by Shailendra Kumar Sah (Roll Number: 063/MSS/R/110), in partial fulfillment for the award of degree of Master of Science in Structural Engineering at Institute of Engineering, Tribhuvan University, Nepal is a record of a bonafied works carried out by him under my supervision and guidance, no part of it has been published or submitted elsewhere for a degree.*

.....

Prof. Dr. P.N. Maskey

Professor

Department of Civil Engineering

Institute of Engineering, Pulchowk Campus,

Tribhuvan University, Lalitpur, Nepal

## **ACKNOWLEDGEMENT**

I express my sense of gratitude to my thesis supervisor, Professor Dr. Prem Nath Maskey for his valuable guidance, critical discussions, continuous encouragement and support during the thesis program. His constant surveillance and suggestions have helped me in the critical stages of the thesis. I am especially indebted to professor Maskey for keeping a special interest on the topic.

I am equally thankful to Dean, Institute of Engineering, Pulchowk campus, Head, Department of Civil Engineering and Dr. Roshan Tuladhar, Program Coordinator, M.Sc. Structural Engineering.

I express my gratitude to C.V.R Murthy, Associate Professor, IIT Kanpur for their valuable suggestion and nice co-operation during our visit IIT Kanpur in search of necessary materials for my research work.

I am very much thankful to my friends Mr. Deepak Kumar Gupta, M.Sc. structural engineering, Mr. Umesh Prasad Chaudhari and all of my class mates for their co-operation during my research work.

Last but not least, I express my gratitude to my parents for their unwavering support and encouragement, without which none of this might have been possible.

Shailendra Kumar Sah

063/MSS/R/110

## **ABSTRACT**

The study on “Earthquake Ground Motion Parameter for Structural Design in Nepal” is carried out in two parts: in the first part, the probabilistic seismic hazard analysis is carried out for the Kathmandu Valley considering 10-active faults as earthquake sources; the recurrence law proposed by Gutenberg-Richter is used. The intensity of earthquake at the center of Kathmandu valley in terms of PGA and SA is obtained by adopting the attenuation law proposed by Youngs et al (1997) and poisson’s process for occurrence of earthquakes. Using conditional probability of magnitude of earthquake and source to site distance, the probabilistic seismic hazard curves are obtain at the bed rock, free field as well as separately assuming soil amplification factor of 2. In the second part of the study, a single envelope of the spectral ordinates are obtained using Young’s et al empirical relationship due to all sources for bed rock and free field separately, which are used to simulate Time-Histories at the bed rock as well at free field . The study shows that the contribution of Source Gosai Kunda (MCT-3.30) in Seismic Hazard curves is larger compare to the other sources and it is considered to be the vulnerable source for Kathmandu City. The program developed in Visual Fortran which generates time history from response spectra and gives good result within 20 iterations. Results are verified using Standard Software (SeismoSignal).

## Table of Contents

Copyright.....	I
Certificate.....	II
Acknowledgement.....	III
Abstract.....	IV
Table of Content.....	V
List of Tables.....	VII
List of Figures.....	VIII
List of Symbols.....	IX
1. INTRODUCTION.....	1
1.1 General.....	1
1.2 Seismicity and geology of Nepal.....	2
1.3 Problem and issues.....	5
1.4 Needs of the study.....	6
1.5 Objective.....	7
1.5.1 Overall objective.....	7
1.5.2 Specific Objectives.....	7
1.6 Scope of the Study.....	7
1.7 Organization.....	8
2. LITERATURE SURVEY.....	12
2.1 General.....	12
2.2 Literature on Recurrence law and Earthquake source modeling.....	12
2.3 A brief description of traditional strong motion attenuation relationships.....	13
2.3.1 Review of Existing Attenuation Relationships.....	14
2.4 Literature on Soil amplification and site geology.....	14
2.5 Literature on shear wave velocity.....	16
2.6 Ground Response Analysis to develop Site-Specific Response Spectra at Soil sites.....	17
3. SEISMIC HAZARD EVALUATION.....	20
3.1 General Approach.....	20
3.2 Probabilistic Seismic Hazard Analysis.....	21
3.3 Identification of Seismic Sources with Characteristics.....	22
3.4 Attenuation Relationship.....	25

3.5 Determination of intensity parameter (PGA) at the bed rock of the site.....	25
3.5.1 Seismic hazard curve .....	27
3.6 Response Spectral Attenuation Functions .....	28
3.7 Numerical Study .....	29
3.8 Results and Discussion .....	29
4. TIME HISTORY SIMULATION .....	36
4.1 General .....	36
4.2 The acceleration time-history of the earthquake in Reference 2 as expressed as .....	36
4.3 Duration and Envelope function .....	39
4.4 Method based on interpolation of excitation .....	40
4.5 Newmark's Method.....	42
4.6 Theoretical Back Ground of SeismoSignal software .....	42
4.7 Numerical Study .....	43
4.8 Result and Discussion .....	44
5. CONCLUSION AND RECOMMENDATIONS .....	56
5.1 General Conclusion.....	56
5.2 Major Conclusion.....	56
5.3 Recommendations .....	57

REFERENCES

Appendix:-



## LIST OF TABLE

<b>Table</b>	<b>Title</b>	<b>Page</b>
Table 1.1	Physical feature of Nepal with geological structure .....	9
Table 1.2	The type and number of faults.....	9
Table 1.3	Arrangement of earthquake events .....	10
Table3.1	Earthquake sources with its characteristics values and probability density function (PDF).....	31
Table 4.1	Weightage average duration for Center of Kathmandu City. ....	45
Table 4.2	COEFFICIENT IN RECURRENCE FORMULAS ( $\zeta < 1$ ) .....	45
Table 4.3	NEWMARK'S METHOD: LINEAR SYSTEMS .....	46

## LIST OF FIGURES

<b>Fig</b>	<b>Title</b>	<b>Page</b>
Fig. 1.1	Fault System and Epicenter of large earthquakes in Nepal. ....	11
Fig. 1.2	Historical earthquakes (points) and faults (line) .....	11
Fig. 3.1	Earthquake Recurrence models by Gutenberg-Richter. ....	32
Fig. 3.2	Variation of PGA with source to site distance for different magnitudes of earthquake for bed rock level. ....	32
Fig. 3.3	Seismic Hazard Curve at Bed rock level for Center of Kathmandu City. ....	33
Fig. 3.4	Seismic Hazard Curve at Free-Field for Center of Kathmandu City. ....	33
Fig. 3.5	Seismic Hazard Curve at Bedrock & Free-Field for Center of Kathmandu City. ....	34
Fig. 3.6	Comparison of Seismic Hazard Curve at Bedrock & Surface for Center of Kathmandu City, assuming soil amplification factor of 2. ....	34
Fig. 3.7	Response Spectra at Bedrock for Center of Kathmandu City. ....	35
Fig. 3.8	Response Spectra at Surface for Center of Kathmandu City .....	35
Fig. 4.1	Intensity envelope function $F(t)$ .....	47
Fig. 4.2	Division of duration and envelope function. ....	47
Fig. 4.3	Simulated Time histories for Center of Kathmandu City at bed rock level. ....	48
Fig. 4.4	Simulated Time - Histories for Center of Kathmandu City. ....	49
Fig. 4.5	Spectral Acceleration for Center of Kathmandu at bed rock level. ....	50
Fig. 4.6	Spectral Acceleration for Center of Kathmandu at Surface level. ....	50
Fig. 4.7	Comparison of Spectral Acceleration using SeismoSignal Software and developed Program. ....	51

## List of Symbols

# 1. INTRODUCTION

## 1.1 General

Nepal lies in highly seismically vulnerable region because of geotectonic activities and the geotechnical condition of the region. A structure to be designed in this region shall consider rationally the seismic risk.

Earthquakes are among the most destructive natural disasters. The life and economic loss which may result from severe earthquake striking a densely populated area, is a direct consequence of damage and collapse of buildings. There are several densely populated mega-cities that are located in a soft deposit and are not far from seismically active faults. As scientifically proven, soft deposit tends to magnify earthquake accelerations several times even if the epicenter distance is several hundreds of Km away as was the case with Mexico City 1985 earthquake. Unless the buildings were designed to resist earthquake forces, such magnified ground acceleration may result in severe damage to buildings causing many fatalities and casualties.

The problem of earthquake resistant design of structural frameworks has been recognized by engineers for many years, but it is only recently (1950's) that the most significant progress has been made. These advances resulted from many factors including: (1) increasing availability of strong ground motion records in some parts; (2) the introduction of statistical approaches in analysis and design; (3) improved understanding of the dynamic behavior of heavily loaded structures; and (4) increasing availability of high-speed digital computers and powerful software for nonlinear dynamics analysis of structures. Unfortunately the availability of strong motion records does not apply to many seismically active areas. An earthquake is usually defined by a collection of responses time history. If the observations can be predicted, the process is called deterministic. If however, the observations can only be defined in terms probability statements, the process is referred to as non-deterministic or stochastic.

The true random nature of earthquake phenomena can be realistically represented only by stochastically mathematical models. Analyses that have used actual recorded data of particulars are equivalent to deterministic. Although the deterministic aspects of these analyses become less restrictive when affects of a large number of past earthquakes are studied, the opportunity to investigate response for spectrum of reconstructed earthquakes is limited by the relatively small number of existing record of strong motion earthquake and their total absence in some cases. These concepts give rise to the use of recommended use of simulated earthquakes time histories to represent ground motion. This thesis focuses to generation of acceleration time histories of earthquake using spectral analysis. Although simulation of earthquakes' time histories becoming less important due to increases in availability of earthquake records and wide spread of strong ground motion accelerograms, this is not the case in many part of the world where there is still moderate earthquake activity rate. Therefore, the necessity and importance of such research stem from the lack of strong ground motion record for Nepal as a large city with moderate seismic activity rate.

Acceleration Time-histories & Response spectrum are the most detailed representation of earthquake ground motion and contain a wealth of information about the nature of the ground shaking. The data are required by engineers or researchers for analyzing the performance of new or existing structures located at a specific site and the response of layered soil deposits under seismic loading. Selection of appropriate time-histories for specific geological and seismological conditions plays an important role for obtaining accurate results.

The present study deals with the simulation of earthquake ground motion for the probabilistic risk assessment of structure. Peak Ground Acceleration, Acceleration Response Spectra, and Ground motion are selected as the parameters to characterize the earthquake ground motions.

## **1.2 Seismicity and geology of Nepal**

The seismicity of Nepal and the surrounding region is attributed to the result of Geotectonic activities in the Himalayan range which is considered to be relatively new. The rock types in the region, in general, are considered to be soft.

Nepal is situated in the central part of the Himalayan arc, and tectonically lies between the Indian and Eurasian Plate. Convergence rate between which is 41 to 61 mm per year as presented by Minster and Jordon in 1978 (Pandey and Molnar 1988).

Nepal takes approximately half length of greater Himalaya, which is part of the trans-alpine belt, regarded as one the main earthquake prone zones of the world and it is located between latitudes 26°22' N to 30°27' N and longitude 80° 04' E to 88° 12' E with an average east-west axis length of about 885 Km and north-south width of 193 Km. The physical feature of Nepal with geological structure from south to the north (Sharma 1997) is presented in Table 1.1. Because of tectonic movement, many earthquakes have occurred in this region in its history. Records noted on some Nepalese religious tracts indicate that a big earthquake hit Kathmandu in June 1255 AD. The quake killed approximately one third of its population at that time. Since then severe earthquakes have been reported which occurred in 1405, 1408, 1681, 1810, 1866 and 1934 AD (BECA 1993, Ambrasseys and Douglas 2004). Evidences in big earthquake in central part of Nepal occurred in the period from 700 to 1100 AD have been published recently but exact occurred date has not conformed yet (Lave et al. 2005). Historical records show that at least as far back as the early 18<sup>th</sup> century, damaging earthquakes have occurred in the Himalayan region in every few decades. But since 1950, the damaging earthquakes have not been reported in this region and in some areas. From recent studies depending upon the various analysis and GIS (Geographical Investigation System) data, slip rate of Indian and Tibetan plates is 19 mm per year (Jouanne et al. 2004). But the calculated slip for the whole Himalayan-arc from occurred earthquakes is only one third of the observed slip (Bilham and Ambrasseys 2005). It shows that either the earthquake records are missing or severe earthquakes may be overdue. Many earthquake struck greater Himalayan region in past but the worst may be yet to come and it may occur in or near Nepal. According to the new analysis by Bilham and Ambrasseys 2005, one or more massive earthquakes measuring greater than M8 on Richter scale may be overdue in the Himalaya, threatening the millions of people that live in the region.

More than ten thousand people were killed in 1934 earthquake. Since then, Nepal's population has doubled and urban population has increased by a factor more than ten

since last greater earthquake. In urban, most of the people live in poorly constructed houses without considering the seismic codes. In rural area almost all people live in low strength masonry house constructed by manly by stone and bricks which have been proved the major cause of live loss in earthquakes. Considering past human tolls from earthquakes, population increases that have occurred since then and the added low quality houses, the future scenario of deaths and damages could be worse than 2005 Pakistan earthquake. Previous seismic hazard estimate (BECA Worley International 1993) is based on uniform distribution of assumed earthquakes data over big area without well explained details. The site consists of 92 faults (BECA Worley International 1993). The types and number of the faults are presented in Table 1.2. The total 197 earthquake events with magnitude greater than M4 are grouped as shown in Table 1.3

Nepal region is composed of different faulting mechanism from Terai to the Himalayan range. Himalayan Frontal Fault (HFF) bound the Terai Plain tectonic area to the north. The Terai plain is composed of alluvial deposits of depth of about 1500m. Churia hill range, composed basically of sandstone, is located to the north of Terai plain and is bounded to the north of by Main Boundary Thrust (MBT) and the HFF respectively. Mahabharat hills and Midland can be categories as Lesser Himalayans (LH) tectonic area. This part is bounded between the MBT and north most Main Central Thrust (MCT). This is mainly composed of schist and Granite in some parts. Higher Himalayan zone including Tethyan Himalayan tectonic area is bounded to the south by MCT and to the north by N-dipping Normal Fault. This area is mainly composed by Gneiss but it also consists of shiest and Gneiss to the upper part but 3.5 to 10km thick section is composed of high- grade metamorphic rock. Inner Himalayan valley includes the Tibetan Plateau which is composed of Tethyan sediment. The fault System and Epicenter of large earthquakes in Nepal is presented in Fig. 1.1. All the faults and historical earthquakes greater than magnitude M3 are presented in Fig.1.2. They are scattered and concerned outside the faults.

The Kathmandu Valley has a long history of earthquakes, but the scientific data of these are remained unrecorded. The seismicity of the valley is basically attributed to its proximity to the Himalayan Range and its peculiar geo-tectonic and geo-technical features. Another major factor influencing the level of ground motion within the

Kathmandu valley is the site amplification due to unconsolidated sediments, which dominates the subsurface soil condition of the valley. With a growing population of almost a million people, uncontrolled development, and building construction techniques that have changed little in the past century, Kathmandu valley has becomes increasingly vulnerable to catastrophic earthquakes with each passing year. To improve the structural performance, improvement in the ability of structure to dissipate the dynamic energy has become a great need of present days. In past years people actually did not used to bother about all these things. But in present days people are showing their interest in constructing seismic resistant structures.

### **1.3 Problem and issues**

As already mentioned, Nepal lies in highly seismically vulnerable region. Therefore, this region has high chances of tectonic earthquake in addition to earthquake through the local slippage of geological faults underneath. Lots of damages have been suffered in Nepal due to past earthquakes. Since no structure can be built as 100% earthquake proof. Considering the importance of structure and compromising economically, structures are designed to withstand certain earthquake of particular level of interest. This necessitates the probabilistic approach to the seismic design of the structures situated at particular location

We are still using mostly ELCENTRO Time history, which is not developed for Nepal. It is mainly, due to not availability of Time history & Response spectrum curve for Nepal. So own Earthquake ground motion Parameters like Peak ground acceleration, acceleration response spectra, and Time History are very important in case of Nepal, which provides large amount of information and makes precise description of a ground motion rather cumbersome. Therefore, the necessity and importance of such research stem from the lack of strong ground motion record for Nepal as a large city with moderate seismic activity rate.

Fortunately, it is not necessary to reproduce each time history exactly to describe the ground motion adequately for engineering purposes. It is necessary, however able to describe the characteristics of the ground motion that are of engineering significance and to identify a number of ground motion parameters that reflect those



characteristics. For engineering purposes, three characteristics of earthquake motion are of primary significance: (i) The amplitude, (ii) frequency content, and (iii) duration of motion. A number of ground motion parameters have been proposed, each of which provides information about one or more of these characteristics. In practice, it is usually necessary to use more than one of these parameters to characterize a particular ground motion.

#### **1.4 Needs of the study**

Prevailing codes provides earthquake parameters in general for a region and not specific for a particular site. So the major problem generally encountered by the structural engineers in the determination of design earthquake for design of a structure so that it could be properly designed to reduce the possible damages due to the earthquake in the future.

The Indian Standard criteria for earthquake resistant design of structure (IS 1893-2002) or the National Building code for Nepal (NBC-105/1994) serve the practical purposes. These codes generally provide seismic coefficients, which are developed from seismic zoning for a whole country. The same seismic coefficient is taken for the earthquake design of structures lying within the same seismic zone. As a matter of fact, topography, earthquake sources, local soil condition, attenuation relationships etc, which describe the ground motion parameter, are different even in smaller area. Hence in order to determine realistic ground motion parameter at a particular site, seismic Hazard analysis (SHA) is carried out. Accordingly Problem and issues are categorized as follow:

1. Nepal lies in the seduction zone of Eurasian Plate with the Indian Plate. Therefore this region has high chance of tectonic earthquake in addition to earthquake through the local slippage of geological faults underneath.
2. Since no structure can built as 100% earthquake proof. Considering the importance of structure and compromising economically, structures are designed to withstand certain earthquake of particular level of interest. This necessitates the probabilistic approach to the seismic design of the structure situated at particular location.

## **1.5 Objective**

### **1.5.1 Overall objective**

The general objective of this research work is to develop suitable Earthquake ground motion parameters for structural design in Nepal, so that it could be properly designed to reduce the possible damages due to the earthquake in the future.

### **1.5.2 Specific Objectives**

The specific objectives of this proposal research work are as follows:

1. Identification of the seismic sources that can have considerable effect on the region under consideration, evaluations of spatial and size uncertainty of seismic sources and identify the suitable recurrence law.
2. Estimation of Peak Ground Acceleration (PGA) for a site and generation of seismic hazard curve.
3. Generation of Response Spectra.
4. Simulation of Time-history.
5. Development of a program to generate Time History from given Response Spectra.

## **1.6 Scope of the Study**

To achieve the above objectives, the study is carried out with the following scope of work:

1. Identification of seismic sources and determination of seismic parameters of the sources.
2. Identification of suitable attenuation law based on different literatures.
3. Probabilistic Seismic Hazard Analysis and determination of seismic hazard curve at bed rock as well as at free-field.
4. Determination of Response Spectra at bed rock as well as at free-field.
5. Simulation of Time-History using a relation given By M.R. Khan

## **1.7 Organization**

The work has been presented in five chapters including this introduction chapter. In second chapter, Literature survey on the attenuation laws based on earthquake sources (EQ), Simulation of time history and its related parameter, soil amplification factor are discussed. Chapter three discusses the numerical part of probabilistic Seismic hazard analysis (PSHA), identification of EQ sources and its characteristic values. Calculation of Peak Ground Acceleration (PGA) and Spectral Acceleration at the bed rock and free-field are discussed. In chapter four simulation of time history and related parameters are studied. A brief summary and conclusion of the study including extended works are presented in last chapter.

**Table 1.1 Physical feature of Nepal with geological structure**

SN	Belt	Width (Km)	Rock Type	Age of Rock
1.	Terai Plain	20-50	Alluvium	Recent
2.	Churia Hills	20-30	Sand stone	Mid-Miocene to Pleistocene
3.	Mahavarat hills	30-40	Granite, Schist	Pre-Cambrian gneiss
4.	Midland	40-60	Granite, Schist	Pre-Cambrian gneiss
5.	Higher Himalaya Zone	10-6	Himal Gneiss	Pre-Cambrian gneiss
6.	Ineer Himalaya Valley	-	Tethyan	Cambrian- Cretaceous

*Source: Sharma (1997)*

**Table 1.2 The type and number of faults**

SN	Fault	Designation	Numbers	Percentage
1.	Normal	N	17	18.90
2.	Reverse	R	36	36.00
3.	Strike-Slip	SS	0	0
4.	Dip-Slip	DS	1	1.08
5.	Other	OS,RL, LL	38	41.42

*Source: Beca Worley International (1993)*

**Table 1.3 Arrangement of earthquake events**

<b>Year</b>	<b>Magnitude</b>						<b>Total</b>
	<b>Start</b>	<b>End</b>	<b>4.0-4.9</b>	<b>5.0-5.9</b>	<b>6.0-6.9</b>	<b>7.0-7.9</b>	
1100	1931	1	2	5	5	2	<b>15</b>
1932	1936	1	2	1	1	1	<b>6</b>
1937	1941		2				<b>2</b>
1942	1946		1				<b>1</b>
1947	1951		1				<b>1</b>
1952	1956		4	2			<b>6</b>
1957	1961		2				<b>2</b>
1962	1966	7	5	1			<b>13</b>
1967	1971	11	3	1			<b>15</b>
1972	1976	13	3				<b>16</b>
1977	1981	12					<b>12</b>
1982	1986	14					<b>14</b>
1987	1991	29	2	1			<b>32</b>
1992	1996	19	1	1			<b>21</b>
1997	2001	23	2				<b>25</b>
2002	2006	16					<b>16</b>
<b>Total</b>		146	30	12	6	3	<b>197</b>

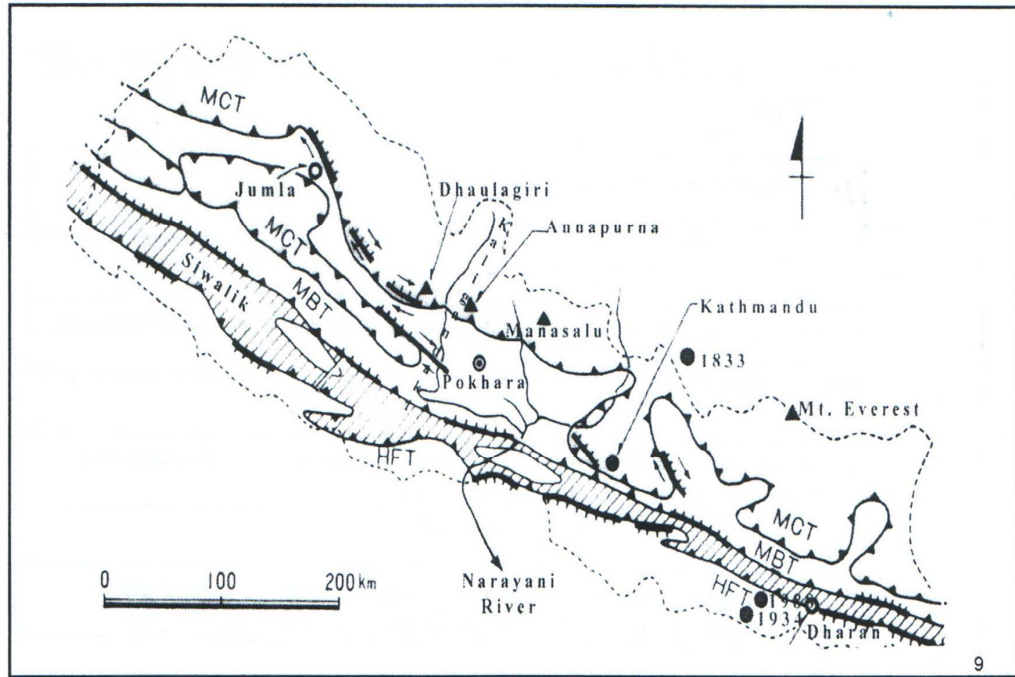


**Fig. 1.1** Fault System and Epicenter of large earthquakes in Nepal.

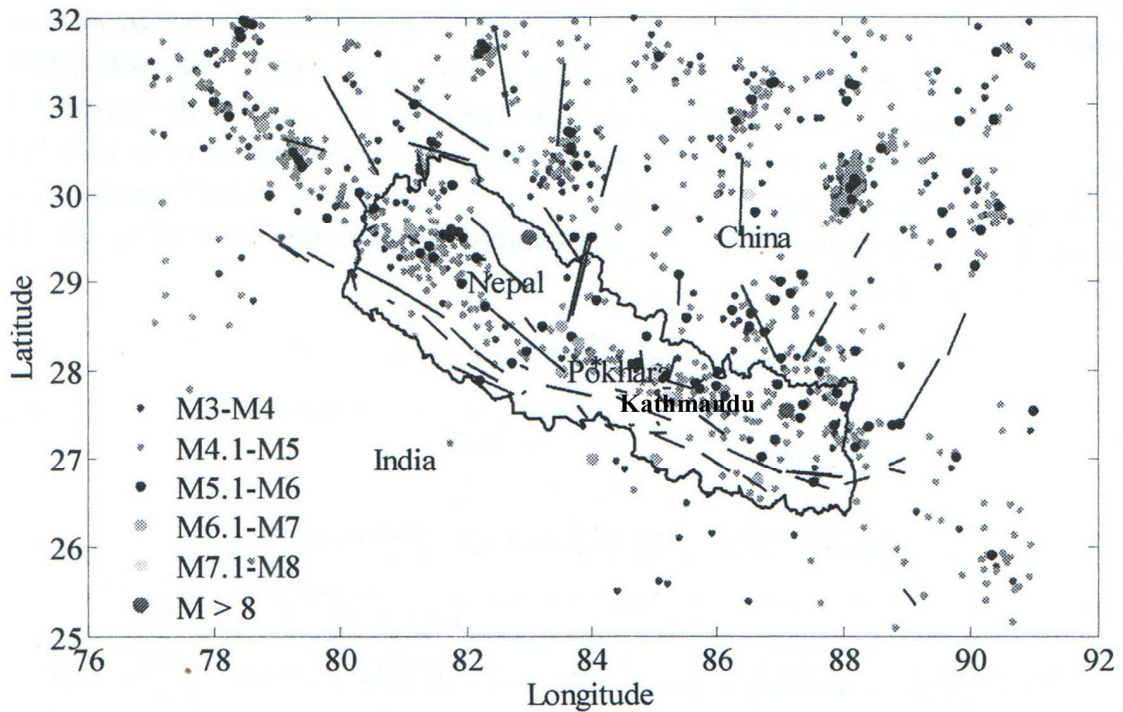


**Fig. 1.2** Historical earthquakes (points) and faults (line)

## 2. LITERATURE SURVEY

### 2.1 General

There are so many excellent literatures are available on the related topic from which some of literatures are referred, however, the literatures for simplicity classified into the broad areas as given below are reviewed to facilitate the study.

### 2.2 Literature on Recurrence law and Earthquake source modeling

On the basis of southern California earthquake records, Guttenberg-Richter (1944) defined the relationship of the annual rate of exceedence of earthquake of certain magnitude with the magnitude itself.

$$\log \lambda_m = a - bm \quad m < m_{\max} \quad (2.1)$$

Where  $\lambda_m$  is the mean annual rate of exceedence of magnitude  $m$ ;  
 $m_{\max}$  is the maximum magnitude occurred in the region;  
 $a$  and  $b$  are statistical constants.

Guttenberg-Richter recurrence law to represent the behavior of single source has been called into question by Schwartz and Cooper Smith (1984) and Schwartz (1988). In a general, stable rate of occurrence of earthquakes are observed in the vicinity of lower and upper magnitude which is not seen in the Gutenberg-Richter recurrence law.

Paleoseismic studies indicate that individual points on faults and fault segments tend to move by approximately the same distance in each earthquake. This has been interpreted to suggest that individual faults repeatedly generate earthquake of similar (within about one-half magnitude unit) size, known as characteristic earthquakes, at or near their maximum magnitude.

Young and Coopersmith (1985) developed a generalized magnitude-frequency density function that combined an exponential magnitude distribution at lower magnitudes with a distribution in the vicinity of the characteristic earthquake. Wesnousky et al. (1984) and Wu et al. (1995) have developed other modes that account for characteristic earthquakes.

Based on five decades of seismicity records for the major seismic sources of southern California, Wesnousky (1994) concluded that while the available data were not sufficient to disprove the Gutenberg-Richter recurrence law. The characteristic earthquake model better represented the observed distribution of earthquake

magnitudes. However, Gutenberg-Richter recurrence law is being widely used by researchers.

### **2.3 A brief description of traditional strong motion attenuation relationships**

Strong motion attenuation relationships have long been an important tool in both Deterministic and probabilistic seismic hazard analysis. In estimating and designing engineered structures for the earthquake hazard at a given site, it is necessary to have relationships describing the expected ground motions at a given site as a function of factors such as source magnitude, distance away from the source, and local site characterization. Almost all attenuation relationships describe expected peak ground motions as functions of earthquake magnitude, a measure of distance to the source region, and local site characterization. In standard regression terminology, the peak ground motion quantities are the dependent variables, and magnitude, distance, and site condition are the independent or predictor variables. Some attenuation relationships include other factors such as style of faulting (Boore, Joyner, and Fumal, 1997) and directivity effects (Somerville et al, 1997) to model the observed data. Typically, the quantities being modeled are peak acceleration, peak velocity, peak displacement, and response spectral quantities. Since it has been observed that there are systematic differences in ground motion characteristics across different tectonic regimes, attenuation relationships are typically characterized as being valid for one of three categories: shallow crustal earthquakes in active tectonic regions, shallow crustal earthquakes in stable continental regions, and subduction zone earthquakes (Abrahamson and Shedlock, 1997). Datasets for such attenuation relationships usually consist of global earthquakes of magnitude 5 and greater. Among the more widely used attenuation relationships are those developed by Boore, Joyner, and Fumal (1993, 1994, and 1997), Abrahamson and Silva (1997), Campbell (1997), and Sadigh et al (1997). The Seismological Research Letters special issue on attenuation relationships (Volume 68, Number 1, Jan/Feb 1997) and a review paper by Campbell (2002) are good sources for more details about more traditional strong motion attenuation relationships.



### 2.3.1 Review of Existing Attenuation Relationships

Seismic hazard assessment may be performed deterministically and probabilistically. Both approaches require the use of ground motion attenuation modes for prediction of ground motion parameters at a site. Most of the attenuation modes are based on statistical analysis of recorded ground motions, which are updated as new strong motion data become available. Some of the prominent empirical attenuation relationships literatures for the calculations of peak ground acceleration (PGA) are reviewed (J. Douglas 2001)

In general, the intensity parameters, such as, PGA at a site is a function of sources to site distance and the magnitude of earthquake. Such relationship is reflected in attenuation relationships.

Esteva (1970) developed an attenuation relationship for West USA for unknown numbers of horizontal records from unknown earthquakes; the approximate source to site distance varies from 15 to 500 Km. The magnitudes of earthquakes is also unknown. But the records are from the soils comparable to stiff clay or compact conglomerate and earthquakes of moderate duration. The ground motion model is

$$A = c_1 \exp(c_2 M) (R + c_3)^{-c_4} \quad (2.2)$$

Where A is in gal,  $c_1 = 1230$ ,  $c_2 = .8$ ,  $c_3 = 25$ ,  $c_4 = 2$  and  $\sigma_{\ln} = 1.02$

And also other existing attenuation relationships to be review, which is briefly discussed in Appendix A

### 2.4 Literature on Soil amplification and site geology.

Generally, attenuation of acceleration refers to the bed rock motion or motion related to geological description of recording stations. The recorded ground motion may be affected by the nature of soil on which the recording station is situated. Mac Murdo (1984) noted that “buildings” situated on rock were not by any means so much affected as those whose foundations did not reach to the bottom of the soil “in the 1819 earthquake in catch, India. In his report on the 1857 Neapolitan earthquake, Mallet (1862) noted the effect of local geologic conditions on damage. Wood (1908) and Reid (1910) showed that the intensity of ground shaking in the 1906 San

Francisco earthquake was related to soil and geologic conditions. A large amplification (as much as factor of two) in accelerations was observed to be associated with shallow deposits for sites located near source of small to moderate earthquakes [Campbell, 1985]. The classification of these sites as rock can significantly increase estimates of strong ground motion if enough of these are included in analysis. The different classification schemes used by researchers divide the site into hard rock, shallow rock, shallow alluvium, deep alluvium, stiff soils, deep cohesion soils, soft soils, etc. The classification is based on the depth of the soil deposit, age of the deposit, shear wave velocity of the medium, etc.

The soil response can be modeled either as a function of peak ground acceleration or by using an amplification factor, which predicts the soil site response based on the corresponding motion in the rock. There are important theoretical reasons why ground surface motions should be influenced by local site conditions. At most sites the density and the s-wave velocity of material near the surface are smaller than at greater depths. If the effects of scattering and material damping are neglected, the conservation of elastic wave energy requires that the flow of energy (energy flux,  $\rho V_s u^2$ ) from depth to the ground surface be constant. Therefore, since  $e$  and  $V_s$  decrease as wave approach the ground surface, the particle velocity ( $u$ ) must increase.

For local site effects, two of the most significant earthquakes were the 1985 Michoacán (Mexico) earthquakes (Stone et al., 1987) and the 1989 Loma Prieta (California) earthquake (Seed et al., 1990). These well-documented earthquakes produced strong motion records at sites underlain by a variety of different subsurface conditions in Mexico City and the San Francisco Bay area. Although the Michoacán earthquake was quite large, its great distance from Mexico City produced accelerations at the rock site Fof only .03g to .04g, whereas in the Lake Zone sites, however, peak accelerations were up to five times greater than those at the rock. Similarly, for the San Francisco Bay area (1989) peak acceleration at Yerba Buena (rock sites) were .06g in the E-W direction and .03g in the N-S direction whereas, in the Treasure Island (soil fill site), peak ground acceleration were .16g in the E-W direction and .11g in N-S direction. Clearly, the presence of soft soils at the Treasure Island site caused significant amplification of the underlying bedrock motion.

Seed et al. (1976) made comparisons of peak accelerations attenuation relationships for sites underlain by different types of soil profiles show distinct trends in amplification behavior. Overall trends suggests that peak accelerations at the surfaces of soil deposits are slightly greater than on rock when peak accelerations are small and somewhat smaller at higher acceleration levels.

Idriss, 1990 developed approximate relationship between peak acceleration on rock and soil sites based on the various ground motion recordings.

The strong ground motion produced by the 17th Oct. 1989 Loma Prieta earthquake in northern California was recorded at over 100 stations generated at different sites with significant different geology (e.g. stiff soil, Soft soil, sedimentary soil). Analysis as carried out by M. Niaxi, C.P. Mortgat and J.F. Schneider (1992) showed that 8 out of 10 soft soil sites display significant amplification relative to stiff soil sites (as much as 300 % for horizontal and 200% for vertical component).

Similarly, Masato Motosaka and Masayuri Nagano (1995) carried out the analysis of amplification characteristics of ground motion in heavily damaged belt zone during 1995 Hyogo –ken Nanbu earthquake in kobe city, japan. Analysis showed that 100% amplification of ground motion was observed as comparison to hard rock ground motion.

## **2.5 Literature on shear wave velocity**

Yutaka Ohta and Noritoshi Got (1976) investigated to systematize empirical equations for the shear wave velocity of soils in terms of four characteristics index i.e. the N-value of the Standard Penetration Test, depth where the soil is situated, geological epoch (age) and soil type (R). Fifteen sets of empirical equation to estimate low strain shear wave velocity theoretically may be obtained by combining the above four indexes. All of these sets were derived by use of about 300 data, and their accuracies were evaluated by means of correlation coefficient was .86. The empirical equation relating the standard penetration N-value to the shear wave velocity provided a correlation of only .72 and is one of the lowest ranking among the 15 sets of equations. One of the empirical equations relating to shear wave velocity with the depth, soil type and geological age was as follows:



b. Selection of rock motions. Appropriate rock motions (either natural or synthetic acceleration time- histories) are selected or developed to represent the design rock motion for the site. If natural time- histories are used, a suite of time- histories that have ground motion characteristics (e.g., peak ground motion parameters, response spectral content, and duration of strong shaking) generally similar to characteristics estimated for the design rock motions are selected. The response spectra for the selected rock motions should, in aggregate, approximately fit or reasonably envelop the design rock spectrum developed for the site. Natural time- histories may be scaled by a factor to improve the match to the design rock spectrum. If synthetic time- histories (i.e., recorded time- histories modified to achieve a match to a smooth response spectrum) are used, their spectra should approximately fit the design rock spectrum. The duration of shaking should also be reasonable. It is desirable that more than one synthetic time- history be used. Preferably, rock motions are assigned at a hypothetical rock outcrop at the site, rather than directly at the base of the soil profile. This is because the knowledge of rock motions is based on recordings at rock outcrops; and unless the rock is rigid, the motions at the base of the soil profile will differ from those of the outcrop. (The differences increase as the ratio of shear wave velocity of rock to shear wave velocity of soil decreases.) Some computer codes allow the rock motion to be assigned as an outcropping motion.

c. Ground response analyses and development of ground surface response spectra. Using the rock time- histories as input motions, ground response analyses are conducted for the modeled soil profile(s) to compute ground motions at the ground surface. Nonlinear soil response is approximated by either equivalent linear analysis methods (e.g., SHAKE (Schnabel, Seed, and Lysmer 1972), or WESHAK (Sykora, Wahl, and Wallace 1992)) or nonlinear analysis methods (e.g., DESRA (Lee and Finn 1985) or SUMDES (Li 1990)). Parametric analyses should be made to incorporate uncertainties in dynamic soil properties. Analyses are generally made for best-estimate (average), upper-bound and lower-bound soil properties. Response spectra of the ground surface motions are calculated for the various analyses made. These response spectra can then be statistically analyzed

and/or interpreted in some manner to develop design response spectra of surface motions. The time-histories obtained from the site response analyses can be used as representative time-histories of surface motions. Because the response spectra of the input rock time-histories may not closely match the rock design response spectrum (particularly when natural time-histories are used), it may be desirable to obtain “site amplification ratios” from the ground response analyses rather than using the response spectra of calculated surface motions directly. Site amplification ratios are ratios of the response spectra of the ground surface motions computed from the ground response analyses divided by the response spectra of the corresponding input rock motions. Statistical analyses can be made on the amplification ratios or some other method used to obtain design amplification ratios. The estimated response spectrum at the ground surface is then obtained by multiplying the site amplification ratios by the design rock response spectrum over the entire period range. A design response spectrum is then developed by further smoothing the estimated ground surface response spectrum as required. The time-histories from the ground response analyses can be used directly to represent ground surface motions, or synthetic time-histories can be developed to match the design ground surface response spectrum.

### 3. SEISMIC HAZARD EVALUATION

#### 3.1 General Approach

Earthquake ground motions, including peak values and time histories, are derived through a process called seismic hazard analysis. Seismic hazard analysis is an effort to estimate what level of ground motion could be expected at a site. Three data sets, earthquake sources (where and how big), earthquake occurrence frequencies (how often), and ground motion attenuation relationship (how strong), are required. In the central and eastern United States, answers to the questions: “where, how big, how often, and how strong?” are very difficult ones. In comparison to typical plate boundary seismic zone such as coastal California, the central and eastern United States is located in the middle of the continent and has a totally different tectonic setting. For example, the exact boundary of the New Madrid Seismic Zone is still difficult to define, even though it is the most active and well studied in the country. The biggest historical earthquake to have occurred in the central United States was the 1811–1812 New Madrid events. The estimated magnitude ranges from about M7 to M8—a large range, though it has been well studied (Johnston, 1996; Hough et al., 2000). Earthquakes are also infrequent, especially large earthquakes that have significant impacts on the built environment. Recurrence intervals for the large earthquakes are quite long, ranging from about 500 years in the New Madrid Seismic Zone to about 4,000 years in the Wabash Valley Seismic Zone; they are even longer in other zones. These recurrence intervals were primarily determined from paleo-liquefaction studies (Tuttle and Schweig, 1996). Several ground motion attenuation relationships are available for the central United States (Campbell, 2003; Frankel et al., 1996; Toro et al., 1997; Atkinson and Boore, 1995; Sumerville et al., 2001). However, all the attenuation relationships were developed based on numerical modeling and sparse strong-motion records from small earthquakes. These attenuation relationships have large uncertainty and predict much higher ground motions in comparison with similar magnitude earthquakes in California.

Two approaches, probabilistic seismic hazard analysis (PSHA) and deterministic seismic hazard analysis (DSHA), are widely used. The two approaches use same data sets, earthquake sources (where and how big), earthquake occurrence frequencies (how

often), and ground-motion attenuation relationship (how strong), but are fundamentally difference in calculations and final results

### **3.2 Probabilistic Seismic Hazard Analysis**

Seismic hazard analysis plays an important role in earthquake resistance design of structures by providing a rational value of input hazard parameter. There can be several parameters to characterizing the hazard levels and there are different methods to estimate those. There are two approaches for estimating the hazard levels; the deterministic approach and the probabilistic approach. Both the approaches have their advantage and disadvantage (Reiter 1990). The deterministic approach is transparent, its input and output parameters are easy to understand (Lindholm and Bungum 2000) , but it does not treat model and data uncertainties. On the other hand, the probabilistic approach correctly refers the actual knowledge of seismicity (orozova and Suhadolc 1999).

The scenario of earthquake is the central concept for the deterministic or maximum credible earthquake (MCR) seismic hazard maps (Anderson 1997), Romeo and Prestininzi 2000. However, when the seismic hazard is influenced by more than one seismic source, it is impossible to define a single scenario earthquake that is compatible with the result of probabilistic seismic hazard assessment (Bomer et al. 2000). Moreover, these are not the bigger earthquakes which always influence the hazard levels; smaller events are also important sometimes due to their higher occurrence rates than those for the bigger events (Wheeler and Mueller 2001). A general rules is that more quantitative the decision to be made is, more appropriate probabilistic hazard and risk assessment would be more over, if many tectonic faults are unidentified seismic sources contribute to the seismic hazard at a site; the integration of those through a probabilistic analysis provides the most useful insight (Mc Guir spectrum (UHS), which is a convenient tool to compare the hazard representations of different sites (Peruzza et al. 200). Since UHS is often the preferred goal of PSHA, any of the spectral properties can be considered as hazard parameter. More over, for the design of important structures, hazard analysis should consider frequency dependent amplification of ground motion associated with the local site



conditions, and in such cases, use of the spectral hazard parameters becomes essential (Mc Guire et al. 2001).

PSHA can be carried out in various ways depending on how one defines the modes of seismicity. Cornell (1968) first introduces the probabilistic seismic hazard analysis (PSHA). He has been the pioneer in developing the procedure for PSHA and is still being used in seismic hazard analysis. The assumptions made are as follows:

- I. Earthquake epicenter is located within the seismic zone.
- II. Within the seismic zone, epicenters are uniformly spatially distributed.
- III. Earthquake occurrences in different seismic source zones are statically independent.
- IV. Earthquakes are randomly distributed with regard to time. The probability distribution of earthquake in time is Poisson's distribution.
- V. Peak ground acceleration (PGA) at a site depends upon earthquake magnitude and source to site distance which describes the attenuation relationship.

There is a certain relationship that exists between the rate of occurrence of earthquake of particular magnitude and rate of the earthquake itself. The concept considers the model of all potential earthquake sources in the region under consideration (Seismic model) and how the intensity of ground shaking will be diminished with distance away from the earthquake occurring within each of the sources (attenuation model). These two are combining to express the probability of exceedence of particular level of ground shaking in certain time interval.

### **3.3 Identification of Seismic Sources with Characteristics**

The essential ingredients of seismicity are the description and location of all the seismic sources likely to affect the region under consideration and an estimate of the likely future recurrence of earthquakes of various magnitudes for each of the sources. The different features of sources can be identified such as fault traces and subduction zones or where there is insufficient definition, the sources can be represented as an area over which seismicity will be similar. While it is relatively easy to identify previous faulting,

it is often difficult to estimate the likely future occurrence of earthquakes which would be associated with future fault activity. Without these recurrence estimates, it is impossible include the faults as specific seismic sources in a probabilistic analysis and recourse must be made to broad aerial sources.

**(i) Spatial Characteristics of fault sources:**

Seismic sources require consideration of spatial characteristics of linear sources and distribution of earthquake within that source zone. A uniform distribution within the source zone does not reflect the uniform distribution of source to site distance. The uncertainty in the source to site distance can be described by probability density function. For the linear source, the probability that earthquake occurs on small segment of fault  $L=l$  to  $L=l+dl$  is the same as the probability that it occurs between  $R= r$  to  $R= r +dr$  [Refer figure 3.1 (a) & b]: that is

$$f_L(l)dl = f_R(r)dr, \tag{3.1}$$

$$f_R(r)dr = f_L(l)dl/dr, \tag{3.2}$$

Where  $f_L = f_L(l)$  and  $f_R = f_R(r)$  are probability density function for variables in  $L$  and  $R$  respectively.

Uniform distribution of  $f_L(l)$  means  $f_L(l) = 1/L_f$

Since

$$l^2 = \sqrt{r^2 - r_{\min}^2}$$

$$f_R = \frac{r}{L_f \sqrt{r^2 - r_{\min}^2}} \tag{3.3}$$

However, it is easier to evaluate  $f_R(r)$  by numerical rather than analytical method. For each linear fault sources to site distance for each segment is calculated at the center of fault i.e. point source, it is the limitation of the assumed attenuation law. The average of the maximum and minimum source to site distance.

**(ii) Size characteristic of fault sources:**

Another aspect is the recurrence relationship for each source. Gutenberg – Richter (1944) recurrence law is adopted here. Statically investigation of historical seismicity

over areas of similar seismicity have shown the relationship between the frequency of occurrence of earthquake greater than or equal in Fig. 3.1 was expressed as

$$\log \lambda_m = a - bm \quad m < m_{\max} \quad (3.4)$$

Where,  $\lambda_m$  is the mean annual rate of exceedence of magnitude  $m$ ;  
 $m_{\max}$  is the maximum magnitude occurred in the region;  
 $a$  and  $b$  are statistical constants i.e. characteristic of source.

$$\lambda_m = 10^{a-bm} = e^{\alpha-\beta m} \quad (3.5)$$

Where  $\alpha = 2.303a$ ,  $\beta = 2.303b$ . This covers the infinite range of magnitude from  $-\infty$  to  $+\infty$ , for practical purposes, small magnitude earthquakes ( $<5$ ) cannot produce significant damages and hence below M5 magnitude are discarded in the hazard analysis. Similarly the upper bound magnitude greater than M9 have never been observed in the past earthquake even in the world. Hence every fault sources are associated with maximum magnitude  $M_{\max}$  which are also adopted from the same report as mentioned above.

Mc Guire and Arabasz 1990, gave mean annual rate of exceedence for lower bound and upper bound earthquake as,

$$\lambda_m = \frac{e^{-\beta(m-m_0)} - e^{-\beta(m_{\max}-m_0)}}{1 - e^{-\beta(m_{\max}-m_0)}} \quad (3.6)$$

And probability density function for Gutenberg – Richter recurrence relationship with upper and lower bound earthquake can be written as,

$$f_m(m) = \frac{e^{-\beta(m-m_0)}}{1 - e^{-\beta(m_{\max}-m_0)}} \quad (3.7)$$

For each source the difference between the lower and upper bound magnitude is divided in such a way that the class interval of the magnitude represents around  $M$ . The computed probability density function for each source is presented in table 3.1 Probability of the magnitude falling in the class interval of magnitudes is calculated using following equations.

$$P[m_l < m < m_u] = f_M(m)dm \approx f_M\left(\frac{m_l+m_u}{2}\right)(m_u - m_l) \quad (3.8)$$

### 3.4 Attenuation Relationship

Attenuation relationship provides the relationship between the level of ground shaking and distance from the earthquake source for varying magnitudes. The level of shaking and distance from the earthquake source for varying magnitudes. The level of shaking are generally interpreted as Modified Mercalli intensity (MMI) and ground motion (acceleration, velocity and displacement). In this study peak ground acceleration as the intensity parameter is used. The uncertainty associated with such attenuation law is large. If this uncertainty is ignored, the hazard result can be erroneous. Therefore, it is necessary to define the distribution of results about the defined mean attenuation predication. There are a number of empirical attenuation relationships developed based on different amount of data of different quality measured from the earthquake occurred in the past in various regions of the world. For the present study attenuation law proposed by Youngs et al (1997) is used which is described below:

#### Attenuation law of Young's et al. (1997)

Young's et al. (1997) developed an attenuation relationship based on the 476 strong motions records from 164 earthquakes that occurred in subduction zones i.e. Alaska, Chile, Cascadia, Japan, Mexico Peru and Solomon islands with magnitude ranging from 5.0 to 8.2 Moments Magnitude ( $M_w$ ). Distance to rupture plane as well as hypo central distance for some data was taken as the distance parameter ranging from 15 Km to 450 Km. Focal depth used in the analysis was between 10 Km to 229 Km. He has noted the large difference between rock and deep soil.

Attenuation Equations Derived by Young et al (1997 are presented in Appendix A

### 3.5 Determination of intensity parameter (PGA) at the bed rock of the site

For a given earthquake occurrence, the probability that a ground motion parameter Y will exceeds a particular value  $y^*$  can be computed using total probability theorem.

$$P[y > y^*] = P[y > y^*/X]P[X] = \int P[y > y^*/X]f_x(X)dx \quad (3.9)$$

Where  $X$  is vector of random variables that influence  $Y$ . In most of the cases the quantities in  $X$  are limited to magnitude  $M$  and distance  $R$ . Assuming that  $M$  and  $R$  are independent, the probability of exceedence can be written as

$$P[y > y^*] = \iint P[y > y^*/m, r] f_x(m) f_r(r) dm dr \quad (3.10)$$

Which is obtained from the attenuation relationship and  $f_M(m)$  and  $f_R(r)$  are the probability density function for the magnitude and distance respectively.

If the site of reference is in a region of  $N_s$  potential earthquake sources, each of which has an average rate of threshold magnitude exceedence,  $v_i = \exp(\alpha_i - \beta_i m_0)$ , then the total average exceedence rate for the region will be given by

$$\lambda_{y^*} = \sum_{i=1}^{N_s} v_i \iint P[y > y^*/m, r] f_{mi}(m_i) f_{ri}(r_k) dm dr \quad (3.11)$$

The individual components of equation (3.11) are for virtually all realistic PSHAs, sufficiently complicated that the integral can be evaluated analytically. Numerical integration, which can be performed which simply divide the possible ranges of magnitude and distance into  $N_M$  and  $N_R$  segments respectively. The average exceedence rate can then be estimated by

$$\lambda_{y^*} = \sum_{i=1}^{N_s} \sum_{j=1}^{N_M} \sum_{k=1}^{N_R} v_i P[y > y^*/m, r_k] f_{mi}(m_j) f_{ri}(r_k) \Delta m \Delta r \quad (3.12)$$

Where, PDF of magnitude

$$m = (m_1 + m_2)/2$$

$$m_j = m_0 + (j - 0.5)(m_{\max} - m_0)/N_M$$

$$r_k = m_{\min} + (k - 0.5)(r_{\max} - r_{\min})/N_R$$

$$\Delta_m = (m_{\max} - m_0)/N_M$$

$$\Delta_r = (r_{\max} - r_{\min})/N_R \quad (3.13)$$

This is equivalent to assuming that each source is capable of generating only  $N < M$  different earthquakes of magnitude at only  $N_R$  different source to site distance,  $R_K$ .

The Equation (3.12) is then equivalent to

$$\lambda_{y^*} = \sum_{i=1}^{N_s} \sum_{j=1}^{N_M} \sum_{k=1}^{N_R} v_i P[y > y^*/m_j, r_k] P[R = r_k] \quad (3.14)$$

The accuracy of the numerical integration procedure increases with increasing  $N_M$  and  $N_R$ .

The established attenuation relationship will give  $\overline{\ln\text{PHSA}}$ .

Using the Standard normal variate  $Z^*$ , we have,\

$$Z^* = \frac{\ln y^* - \overline{\ln\text{PHSA}}}{\sigma_{\log y}} \quad (3.15)$$

Where is the uncertainty associated with the attenuation relationship, which represents the standard deviation of the lognormal PGA. Using the table of standard variate, we get,

$$P[\text{PHSA} > y^* / M = m_j r_k] \quad (3.16)$$

And then it is possible to calculate which are to be summed for each source to site distance, each magnitude and each source zone.

### 3.5.1 Seismic hazard curve

The seismic hazard curve can be easily combined with the Poisson's model to estimate the probabilities of exceedence in finite time period. The temporal occurrence of EQ is most commonly described by a poisson's model. The Poisson's model provides a sample framework for evaluating probabilities of events that follow a Poisson's process. Poisson's process is based on the following assumptions:

- (i) The number of occurrences in one time interval is independent of the number that occurs in any other non-overlapping time interval.
- (ii) The probability of occurrence during a very short time interval.

The probability of more than one occurrence during a very short time interval is negligible.

The probability of exceedence of  $y^*$  in time period T is,

$$P[y_T > y^*] = 1 - e^{-\lambda_{y^*} T} \quad (3.17)$$

The mean annual rate of exceedence that has certain % probability of exceedence in T year's period will be given by rearranging the above equation.

$$\lambda_{y^*} = \frac{\log(1-P[y_T > y^*])}{T} \quad (3.18)$$

It is often necessary to compute the value of ground motion parameter corresponding to a particular probability of exceedence in a given time period. Reading out from the hazard curve for mean annual rate of exceedence in a given time period can be evaluated.

As a result of PSHA seismic hazard curves at the bed rock is obtained for individual source zone and combined to express aggregate hazard for particular site. The basic concept of the computation requires for the development of seismic hazard curves is fairly simple. The probability of exceeding a particular value,  $y^*$  of a ground motion parameter, Y is calculated for one possible earthquake at one possible source location and then multiplied by that particular magnitude earthquake would occur at that particular location. The process is repeated for all possible magnitudes and locations with probabilities of each source.

### **3.6 Response Spectral Attenuation Functions**

Response spectral attenuation functions express the key response spectrum parameter values as functions of M, R site soil classification and faulting mechanism. The spectral attenuation functions are used to weight the contributions of various earthquake sources to the site seismic hazard, and are seldom used as end-products in their own right. However, if spectral attenuation functions representing the defined range of natural periods are used collectively to derive a design response spectrum for any given combination of M, R and site classification, the “collective function” effectively becomes a pseudo-deterministic response spectrum. Such a pseudo-deterministic response spectrum can model only the average effects of the M, R and site classification and does not take into account any particular source or path effects. Thus, strictly speaking, the response spectrum derived from the spectral attenuation function is only partially deterministic (hence the description “pseudo”), to distinguish it from the fully deterministic response spectrum.

### 3.7 Numerical Study

As there exists certain relationship between the rate of occurrence of earthquake of particular magnitude and the rate of the earthquake itself. The concepts considers the modal of all potential earthquake sources in the region under consideration (Seismicity modal) given in the ‘Seismic Hazard Mapping and Seismic Risk Assessment for Nepal’ as a part of National Building Code for Nepal (Habital) Subproject NEP/88/054. The 10- different sources HFF-1.10 (Narayani River), HFF-1.15 (Dhalkebar) , MBT-2.3 (Arun g Kh), MBT-2.5, ( Hetauda), MCT-3.3 (Gosai Kunda), HFF-1.13 (Amelkhgunj), LH-4.10 (Sunkoshi) and LH-4.7, (Saptakoshi-Deomai) are taken for the research work as shown in tabular form in Table 3.1. The characteristics values, assumed maximum magnitude and moment magnitudes for 10-different sources are taken from the project 88/054. The source to site distance is found from map.

After finding the seismic sources characteristics, maximum magnitude, and source to site distance the annual rate of occurrence of threshold magnitude i.e. 4.5 is determined using the recurrence law given in equation (3.5). The probability density function is calculated using equation (3.16). Then the conditional Probability of exceedence is calculated. Using attenuation law derived by Young’s et al (1997), mean annual rate of exceedence is determined and finally the seismic hazard curve is plotted. All calculations necessary for the PSHA is done in my thesis work under the supervision of my guide and the necessary graph is plotted .i.e. the probability of exceedence versus peak ground acceleration (PGA) as shown in Fig. (3.3 to 3.6). Some calculations with the characteristic values and the assumed maximum magnitude for 10-different sources are presented in tabular form in Table 3.1. Also Using Young’s empirical relationships Spectral Acceleration for rock and soil cases are obtained .The necessary graphs are plotted i.e. Spectral Acceleration (g) versus Period (s) as shown in Fig. (3.7 to 3.8).

### 3.8 Results and Discussion

The seismic characteristic of 10-faults in the vicinity of Kathmandu Region considered in the study as earthquake sources is presented in table 3.1. The same table shows the rate of occurrence of earthquake of magnitude greater than the threshold for



each fault also. The obtain probability density function (PDF) of various magnitude for each fault is worked out in the same table. The Variation of the intensity Parameter (PGA) with source to site distance for different magnitudes calculated considering attenuation law. Fig.3.2. Presents such a curve for magnitudes M5, M6, M7, M8 and M9 using attenuation law proposed by Youngs et al (1997). The intensity parameter reduces as the source to site distance increases. The seismic hazard for the bed rock, free-field and also for soil amplification factor of 2 for center of Kathmandu City using attenuation law Young's et al (1997) are shown in Fig. 3.3, Fig. 3.4 and Fig. 3.6 respectively. The Seismic Hazard curve at bed rock, free field and for soil amplification factor of 2 using the same attenuation law for 50 years are shown in Fig. 3.3, Fig. 3.4 and Fig. 3.6 respectively. The spectral ordinates are obtained for bed rock and free field by Young's empirical relationship separately, which are shown in Fig. 3.7 & 3.8 respectively.

The PGA value for 10% probability of exceedence in 50 years (the corresponding return period is equal to 475 years) using attenuation law by Youngs et al (1997) gives .32g for bed rock where as .39g for free-field. Fig.3.6 shows that for soil amplification factor of 2, the PGA value for 30% probability of exceedence in 50 years is equal to .32g. Fig. 3.7 and 3.8 shows the response spectrum due to individual sources and Single envelope of Spectral Acceleration on the basis of contribution of each source in SHA for bed rock and free-field respectively. Peak of Spectral Acceleration is equal to 0.42g and 0.70g for bed rock and free-field respectively.

**Table 3.1****Earthquake sources with its characteristic values and probability density function (PDF)**

Sources Zone	EQ Sources (Faults)	Fault Name	Fault Type	Assumed $M_{max}$	a- Value	b- Value	Sources-to-site Distance (Km)	Probability Distribution Function (PDF)				
								M5	M6	M7	M8	M9
1	HFF-1.10	Narayni River	R/RL	6.7	5.2	1.5	84	0.7327	0.0732	0.0073	0.0007	0.0001
2	HFF-1.15	Dhalkebar	R	7.2	5.2	1.5	109	0.0732	0.0073	0.0007	0.0001	0.7296
3	MBT-2.3	Arun Kh.	R,N down	7.5	5.2	1.5	171	0.0073	0.0007	0.0001	0.7296	0.0729
4	MBT-2.4	Narayni	R	7.0	5.2	1.5	82	0.0007	0.0001	0.7296	0.0729	0.0073
5	MBT-2.5	Hetauda	R	7.3	5.2	1.5	42	0.0001	0.7296	0.0729	0.0073	0.0007
6	MCT-3.3	Gosai Kunda	R	7.6	5.2	1.5	18	0.7287	0.0728	0.0073	0.0007	0.0001
7	HFF-1.13	Amlekhgunj	R	7.0	5.2	1.5	54	0.0728	0.0073	0.0007	0.0001	0.7304
8	LH-4.10	Sunkoshi-Roshi Kh.	Rt-lat-st-sl	7.0	5.2	1.5	70	0.0073	0.0007	0.0001	0.7304	0.0730
9	MBT-2.6	Udaipur-Sunkoshi	Rev.norm	8.0	5.2	1.5	138	0.0007	0.0001	0.7304	0.0730	0.0073
10	LH-4.7	Saptakoshi-Deomai	R	7.5	5.2	1.5	223	0.0001	0.7304	0.0730	0.0073	0.0007

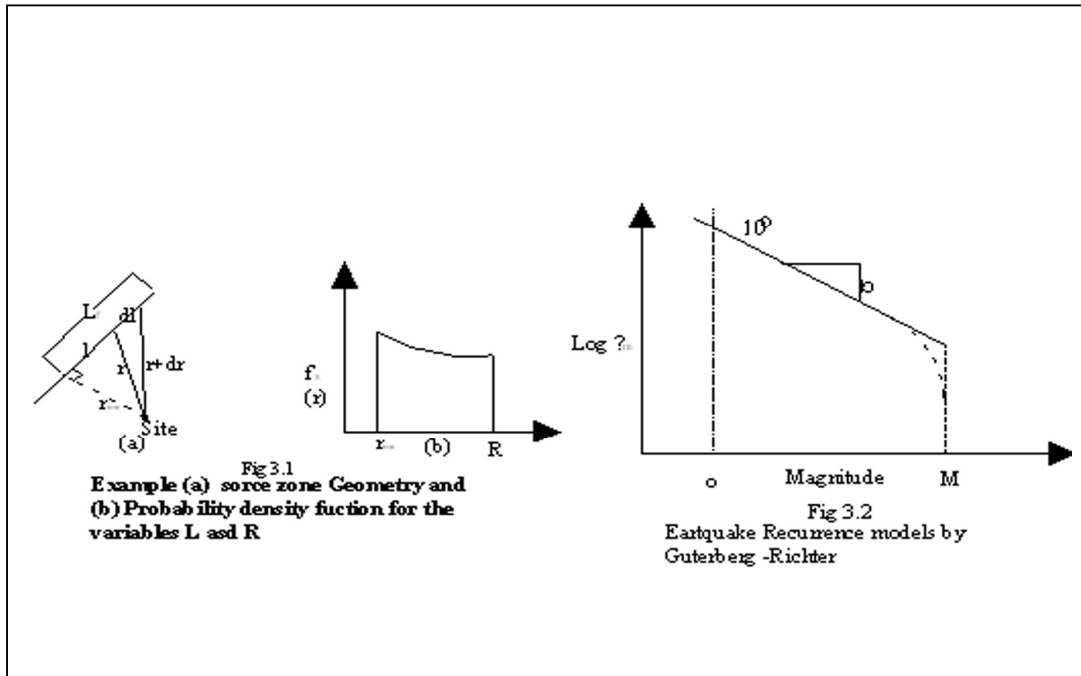


Fig. 3.1 Earthquake Recurrence models by Gutenberg-Richter.

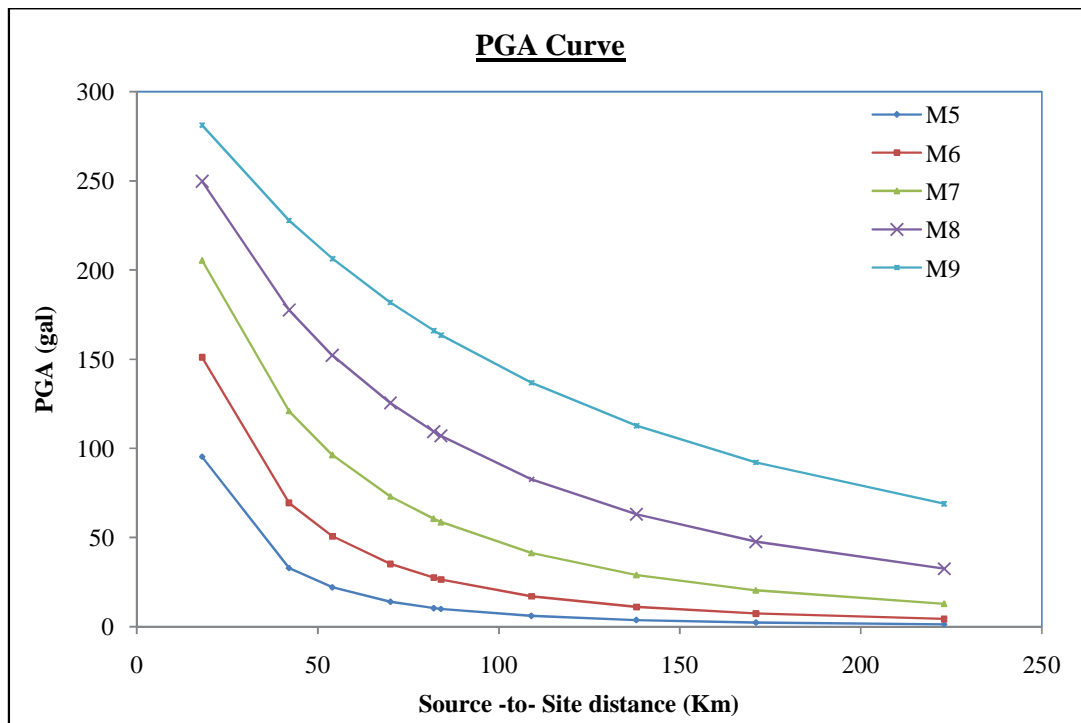
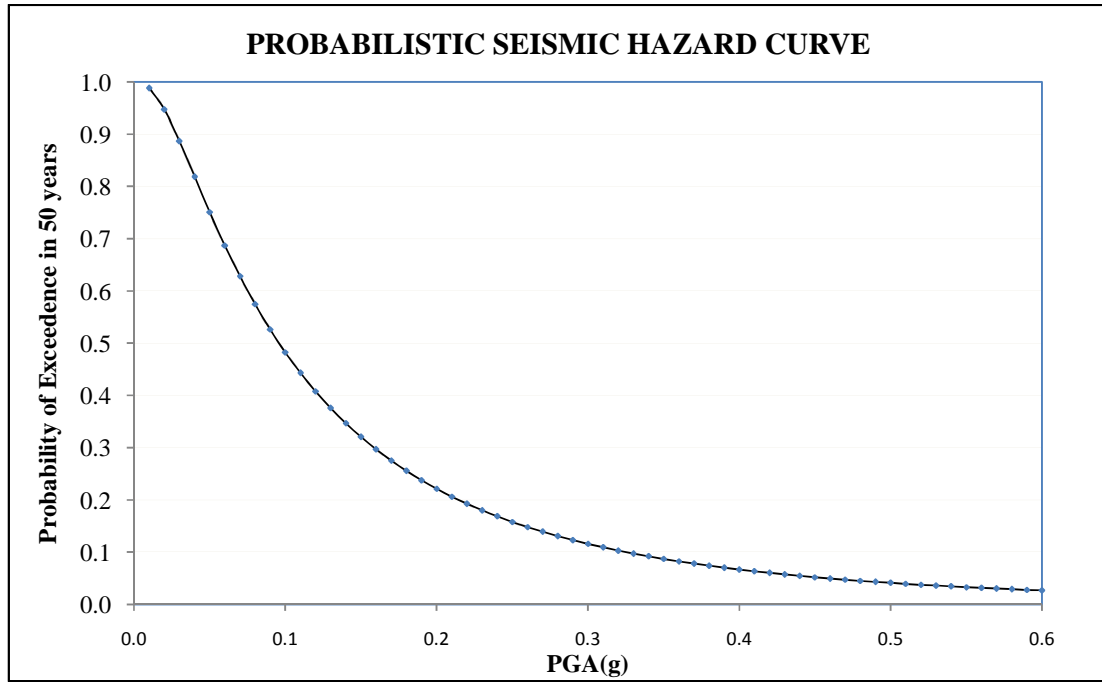
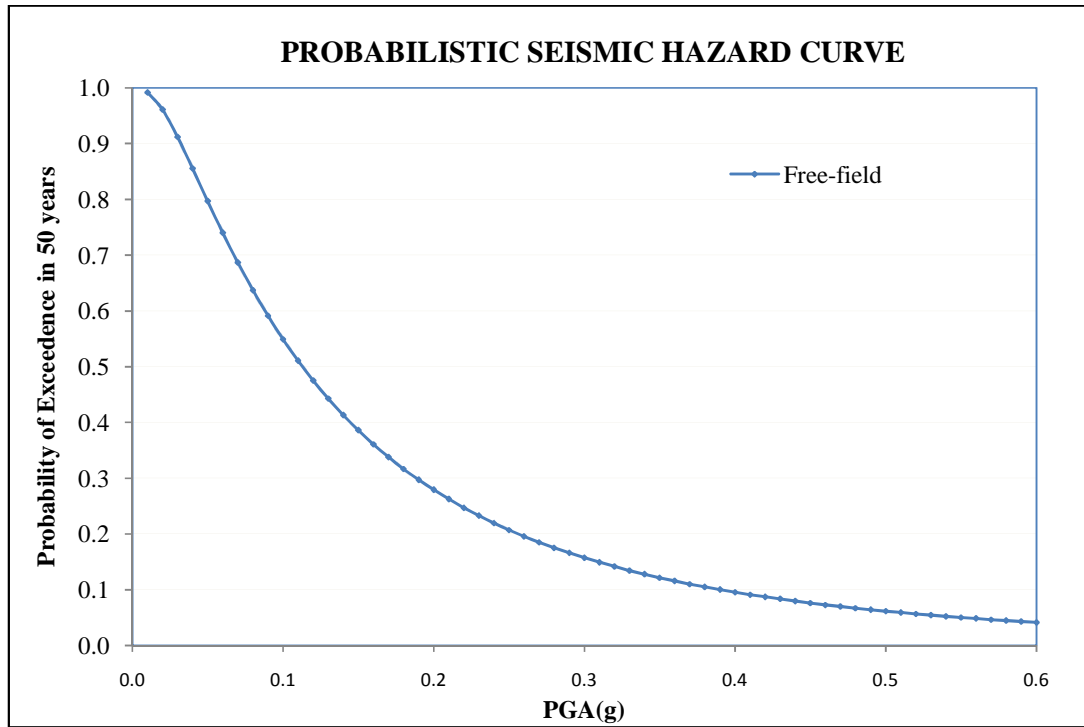


Fig. 3.2 Variation of PGA with source to site distance for different magnitudes of earthquake for bed rock level.



**Fig. 3.3 Seismic Hazard Curve at Bed rock level for Center of Kathmandu City.**



**Fig. 3.4 Seismic Hazard Curve at Free-Field for Center of Kathmandu City.**

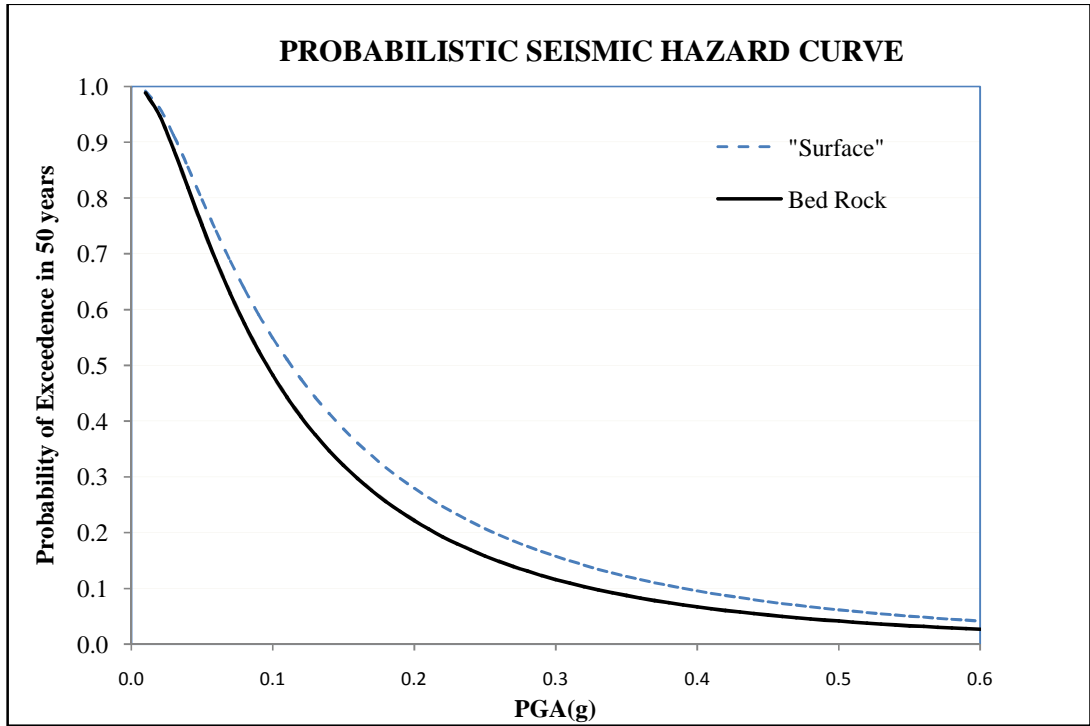


**Fig. 3.5 Seismic Hazard Curve at Bedrock & Free-Field for Center of Kathmandu City.**

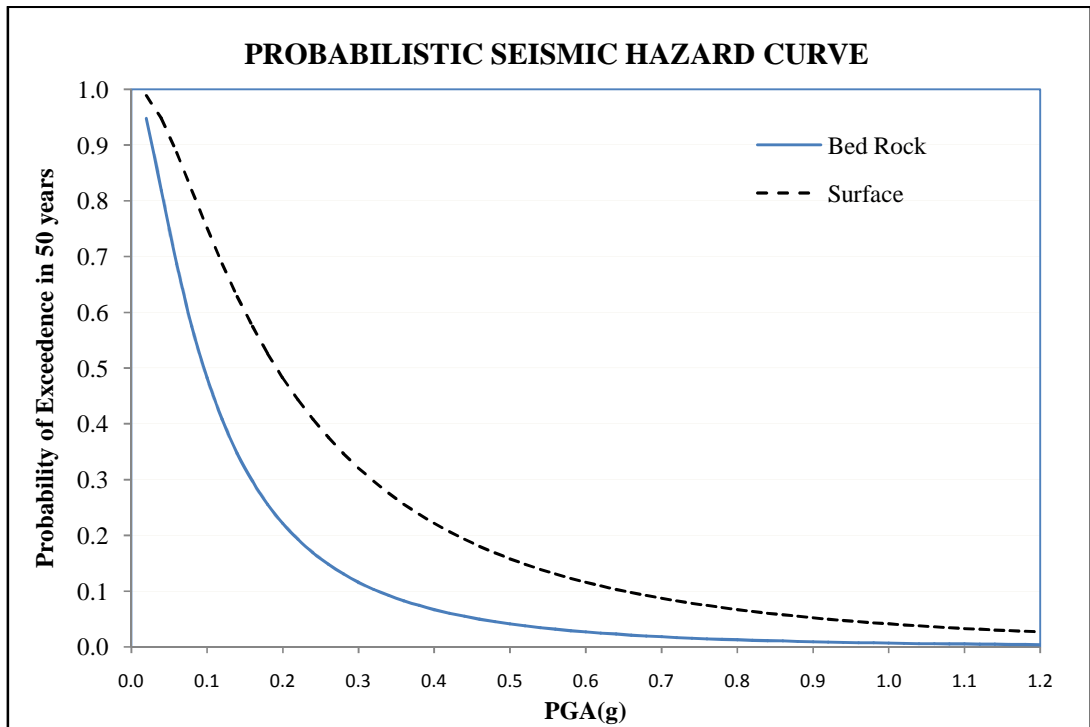


**Fig. 3.6 Comparison of Seismic Hazard Curve at Bedrock & Surface for Center of Kathmandu City, assuming soil amplification factor of 2.**

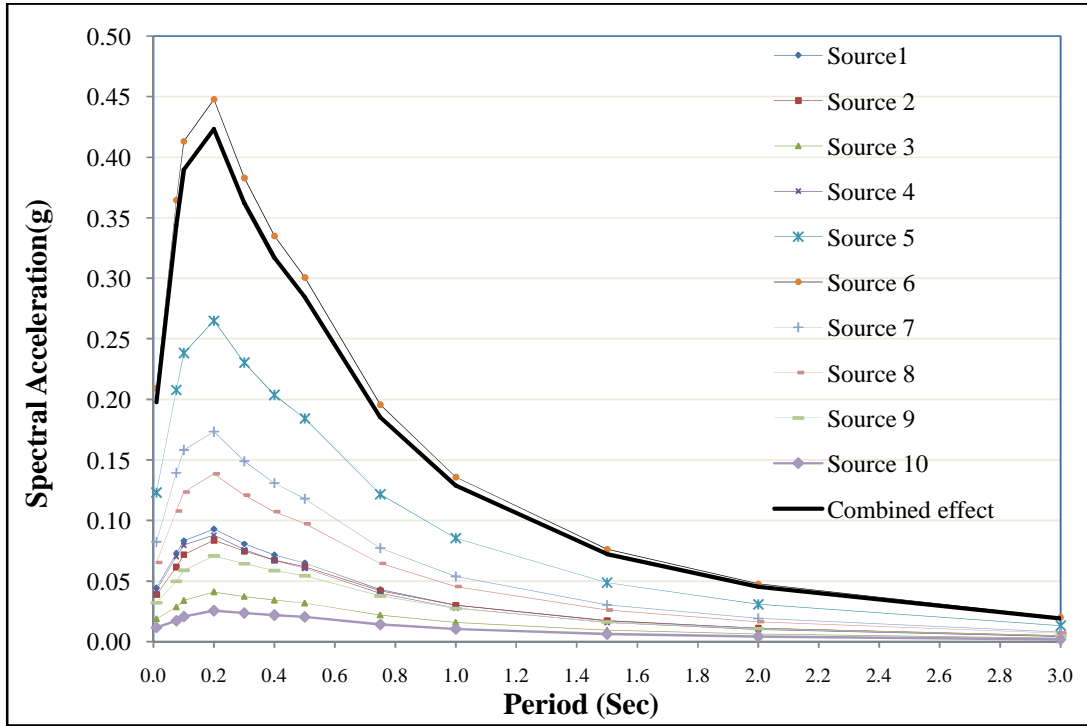


**Fig. 3.7 Response Spectra at Bedrock for Center of Kathmandu City.**

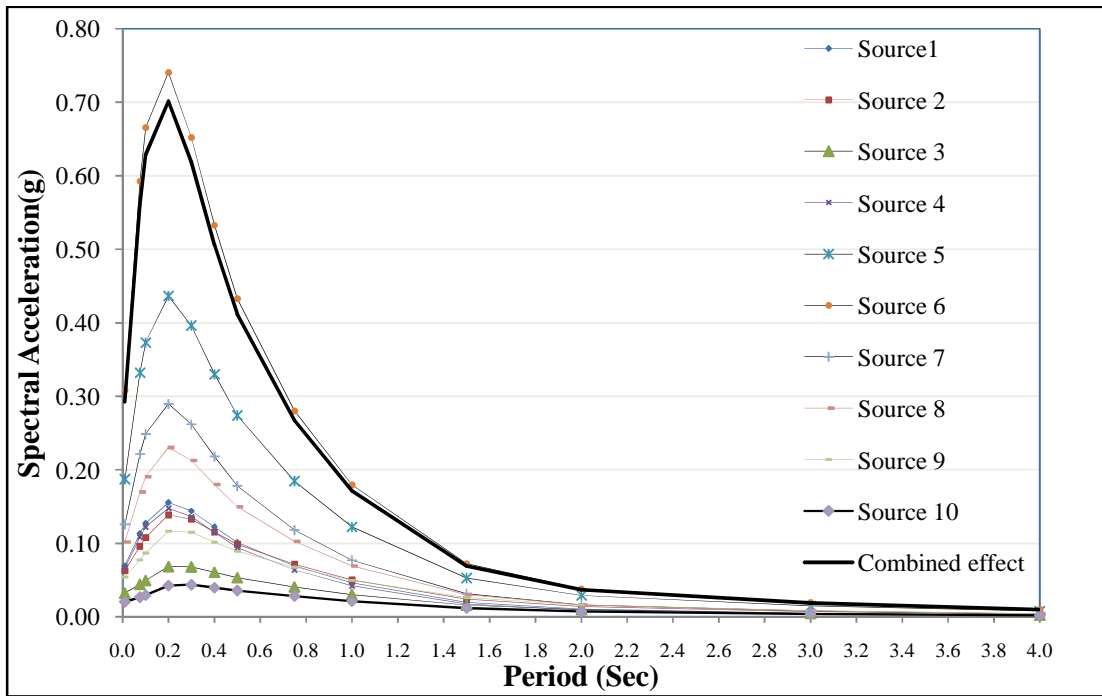


**Fig. 3.8 Response Spectra at Surface for Center of Kathmandu City**

## 4. TIME HISTORY SIMULATION

### 4.1 General

In reference with the hazard curve and response spectrum obtained in chapter 3, seismic input parameters, especially artificial time - history is simulated for design purpose in the region.

### 4.2 The acceleration time-history of the earthquake in Reference 2 as expressed as

$$H(t) = F(t) \times \sum_{i=1}^N (-1)^i A_i \sin(2\pi f_i t) \quad (4.1)$$

Where,  $A_i$ 's are unknown coefficients to be determined,  $F(t)$  is a positive envelope function to the real earthquake (e.g. typical envelope functions such as the boxcar, trapezoidal and exponential, as shown in Fig. 4.1 below can be used),  $N$ =total number of frequencies required to cover the entire frequency range,  $(f_i)$  frequency in cycles per second. The  $A_i$ 's are assumed to vary linearly in magnitude between frequencies at which the desired response spectrum is given.

#### 1. Determination of unknown coefficients ( $A_i$ 's)

The procedure to determine the unknown coefficient  $A_i$  in equation (4. 1) is described in the following steps.

a) From the given floor spectra, initially assume

$$A^v_i(f_i) = C\beta S_a(f_i) \quad (4.2)$$

Where,  $A^v_i(f_i)$  coefficient at frequency  $f_i$ ,  $C$ =constant between 1 to 2 (choose 1.5),  $\beta$ =damping ratio (should be greater than zero),  $S_a(f_i)$  = required or target response spectrum value at frequency  $f_i$ ,  $v$  = iteration number.

Note that constant  $C$  which determines the initial or starting time-history can be safely chosen to have any value from 4.1 to 4.2. The final time history generated are not significantly affected if  $C$  chosen from this range. However, the total number of iterations required for convergence may vary slightly. A value of  $C=1.5$  appears to be an optimum value.

- b) With the envelope function  $F(t)$  and the  $A_i^v$  known, the acceleration time-history in the iteration can be obtained as

$$H^v(t) = F(t) \sum_{i=1}^n (-1)^i A_i^v \sin(2\pi f_i t) \quad (4.3)$$

- c) The response spectra  $S_c(f_i)$  at any frequency  $f_i$  are then calculated using the following equation of motion of a single degree of freedom system:

$$\frac{d^2(x+x_g)}{dt^2} + 2\beta\omega_i \frac{dx}{dt} + \omega_i^2 x = 0 \quad (4.4)$$

Where,  $x_g$  = ground displacement,  $x$  = relative displacement,  $\omega_i$  = frequency (rad/Sec)  
 $= 2\pi f_i$

$$\frac{d^2(x_g)}{dt^2} = H(t) \quad (4.5)$$

- d) The coefficient  $A_i(f_i)$  for the  $(v+1)^{th}$  iteration are obtained as

$$A_i^{v+1}(f_i) = \left( \frac{S_a(f_i)}{S_c(f_i)} \right)^\zeta A_i^v(f_i) \quad (4.6)$$

Where,

$S_a(f_i)$  = Target response acceleration at frequency  $f_i$

$S_c(f_i)$  = Calculated response acceleration at frequency  $f_i$

$\zeta$  = a relaxation parameter the controls the speed of convergence.

The program assume the value of  $\zeta$  to be equal to 1.15 and in all cases the program give excellence convergent results in only 8 iterations.

- e) The iterative process is sopped when the ratio  $\frac{S_a(f_i)}{S_c(f_i)}$  is close to unity at all frequencies or the maximum number of iterations allowed is reached. Otherwise steps (b) to (c) repeated.



## 2. Determination of sine terms (N)

In reference 3, the minimum number of sine terms (N) between starts and end frequencies ( $f_1$  and  $f_2$ ) was selected using the following equation:

$$N = \log_e \left( \frac{f_2}{f_1} \right) / \log_e(1 + .02\beta) \quad (4.7)$$

This selection was such that the half power points of adjacent frequencies overlap. For the majority of the problem, this selection method is adequate. However, it is felt that equation (4.7) could be modified slightly to give more sine terms for damping values higher than 1%. The modified equation (4.8) to be used in this research

$$N = \beta \log_e \left( \frac{f_2}{f_1} \right) / \log_e(1 + .02\beta) \quad (4.8)$$

## 3. Correction for the ground acceleration time histories(base line Correction):

The Time – History generated at each iteration can be modified to have zero final ground velocity and displacement (at time  $t=t_1$ ) by adding a correction term ( $At+Bt^2$ ) to the ground acceleration as follows:

$$\ddot{X}_g = H(t) = F(t) \sum_{i=1}^n (-1)^i A_i \sin 2\pi f_i t + At + Bt^2 \quad (4.9)$$

$$H(t) = H_1(t) + At + Bt^2$$

$$\dot{X}_g = \int_0^t H_1(t) dt + \frac{At^2}{2} + \frac{Bt^3}{3} \quad (4.10)$$

$$X_g = \int \dot{X}_g dt = \int_0^t \int_0^t H_1(t) dt dt + \frac{At^3}{6} + \frac{Bt^4}{12} \quad (4.11)$$

The constant A and B are evaluated by applying the boundary conditions such that the final ground velocity and displacement are zero.

$$\text{Let } \dot{X}_g(t = t_1) = X_g(t = t_1) = 0$$

$$C_1 = \int_0^{t_1} H_1(t) dt; C_2 = \int_0^{t_1} \int_0^{t_1} H_1(t) dt dt$$

The boundary conditions reduce equation (4.10) and (4.11) to

$$\frac{At_1^2}{2} + \frac{Bt_1^3}{3} = -C_1 ; \frac{At_1^3}{6} + \frac{Bt_1^4}{12} = -C_2$$

Solving for constant A and B, we get

$$A = \frac{6}{t_1^3} (C_1 t_1 - 4C_2); B = \frac{12}{t_1^4} (3C_2 - 4C_1 t_1)$$

Therefore correct ground acceleration can be obtained by substituting the values of constants A and B in Equation (4.9)

It must be noted that when these end boundary conditions are applied in ever iteration the do not exactly enforce the final ground velocity and displacement zero in the next iteration. The artificial time –history of last iteration give small value of end velocity and displacement. Sometimes it is very essential to enforce the boundary condition on the end displacement.

### 4.3 Duration and Envelope function

Duration of earthquake is function of magnitude and epicentral distance, thus each earthquake has separate duration. A probabilistic spectrum consists of many earthquakes. Even within duration span acceleration amplitudes are not uniform. Thus total duration ( $T_D$ ) is divided into three parts as shown in Fig. 4.2 In the past up to  $T_B$  acceleration will be ascending, between  $T_B$  to  $T_C$ , it is much effective and after  $T_C$ , it starts descending.  $T_B$  and  $T_C$  are calculated using equations following Osaki 1994 and  $T_D$  is calculated following Kempston and Stewart 2006. It is significant duration which is defined as time interval across which 5 to 95% of total energy is dissipated.

$$T_B = [0.12 - 0.04(M - 7)]T_D \quad (4.12)$$

$$T_C = [0.05 - 0.04(M - 7)]T_D \quad (4.13)$$

$$\ln T_D = \ln \left[ \frac{\left( \frac{\exp(b_1 + b_2(M-6))}{10^{1.5M+16.05}} \right)}{4.9 * 10^6 \beta} + c_2 r + c_1 s \right] \quad (4.14)$$

Where,  $b_1$ ,  $b_2$ ,  $c_1$ ,  $c_2$  are coefficients equal to 2.79, 0.82, 1.91, 0.15 respectively,  $\beta$  is shear wave velocity equal to 3.2 Km/sec.  $s$  is soil type and equal to 1 for soil, and zero for rock,  $M$  is magnitude of earthquake and  $r$  is epicentral distance. Now envelop function  $F(t)$  is calculated using equations (4.15-4.17).

$$0 \leq t \leq T_B: F(t) = \left( \frac{t}{T_B} \right)^2 \quad (4.15)$$

$$T_B \leq t \leq T_C: F(t) = 1 \quad (4.16)$$

$$0 \leq t \leq T_D: F(t) = \exp \left( \frac{\ln 0.1}{T_D - T_C} (t - T_C) \right) \quad (4.17)$$

In order to find out appropriate duration, separate significant durations for all sources using equations 4.12-4.14 were calculated, then obtain durations are multiplied by corresponding cells weight and obtained durations are found summing up all durations. Then weighted average duration are presented in Table 4.1

The Duration of strong ground motion increases with increasing earthquake magnitude. However, the manner in which strong motion duration varies with distance depends on how it is defined. Duration of earthquake represented by Hisada's Equation is

$$T = 10^{.31M-0.774} \quad (4.18)$$

Where, M= Magnitude, T: Duration (sec)

**Envelope Curve:**

Initial: 10% of total T

Main: 40% of total T

Decreases: 50% of total T

**4.4 Method based on interpolation of excitation**

A highly efficient numerical procedure can be developed for linear systems by interpolating the excitation over each time interval and developing the exact solution. If the time intervals are short, linear interpolation is satisfactory. Over the time interval  $t_i \leq t \leq t_{i+1}$ , the excitation function is given by

$$p(\tau) = p_i + \frac{\Delta p_i}{\Delta t_i} \tau \quad (4.19)$$

Where,

$$\Delta p_i = p_{i+1} - p_i \quad (4.20)$$

and the time variable  $\tau$  varies from 0 to  $\Delta t_i$ . For algebraic simplicity, we first consider systems without damping; later, the procedure will be extended to include damping. The equation to be solved is

$$m\ddot{u} + ku = p_i + \frac{\Delta p_i}{\Delta t_i} \tau \quad (4.21)$$

The response  $u(\tau)$  over the time interval  $0 \leq \tau \leq \Delta t_i$  is the sum of three parts: (1)

free vibration due to initial displacement  $u_i$  and velocity  $\dot{u}_i$  at  $\tau = 0$ , (2) response to step force  $p_i$  with zero initial conditions, and (3) response to ramp force  $\left(\frac{\Delta p_i}{\Delta t_i}\right)\tau$  with zero initial conditions.

$$u(\tau) = u_i \cos \omega_n \tau + \frac{\dot{u}_i}{\omega_n} \sin \omega_n \tau + \frac{p_i}{k} (1 - \cos \omega_n \tau) + \frac{\Delta p_i}{k} \left( \frac{\tau}{\Delta t_i} - \frac{\sin \omega_n \tau}{\omega_n \Delta t_i} \right) \quad (4.22)$$

and

$$\frac{\dot{u}(\tau)}{\omega_n} = -u_i \sin \omega_n \tau + \frac{\dot{u}_i}{\omega_n} \cos \omega_n \tau + \frac{p_i}{k} \sin \omega_n \tau + \frac{\Delta p_i}{k} \frac{1}{\omega_n \Delta t_i} (1 - \cos \omega_n \tau) \quad (4.23)$$

Evaluating these equations at  $\tau = \Delta t_i$  gives the displacement  $u_{i+1}$  and velocity  $\dot{u}_{i+1}$  at time  $i+1$ ;

$$u_{i+1} = u_i \cos \omega_n \Delta t_i + \frac{\dot{u}_i}{\omega_n} \sin \omega_n \Delta t_i + \frac{p_i}{k} [1 - \cos(\omega_n \Delta t_i)] + \frac{\Delta p_i}{k} \frac{1}{\omega_n \Delta t_i} [\omega_n \Delta t_i - \sin(\omega_n \Delta t_i)] \quad (4.24)$$

$$\frac{\dot{u}_{i+1}}{\omega_n} = -u_i \sin \omega_n \Delta t_i + \frac{\dot{u}_i}{\omega_n} \cos \omega_n \Delta t_i + \frac{p_i}{k} \sin(\omega_n \Delta t_i) + \frac{\Delta p_i}{k} \frac{1}{\omega_n \Delta t_i} [1 - \cos(\omega_n \Delta t_i)] \quad (4.25)$$

These equations can be rewritten after substituting Eq. (4.20) as recurrence formulas;

$$u_{i+1} = Au_i + B\dot{u}_i + Cp_i + Dp_{i+1} \quad (4.26)$$

$$\dot{u}_{i+1} = A'u_i + B'\dot{u}_i + C'p_i + D'p_{i+1} \quad (4.27)$$

Repeating the derivation above for under critically damped systems (i.e.  $\zeta < 1$ ) shows that equations (4.26-4.27) also apply to damped systems with the expression for the coefficients A, B,.....D' presented in Table 4.2 below. They depend on system parameters  $\omega_n, k$  and  $\zeta$  and on the time interval  $\Delta t \equiv \Delta t_i$ .

Since the recurrence formulas are derived from exact solution of the equation of motion, the only restriction on the size of the time step  $\Delta t$  is that it permits a close approximation to the excitation function and that it provides response results at closely spaced time intervals so that the response peaks are not missed. This numerical procedure is especially useful when the excitation is defined at closely spaced time intervals- as for earthquake ground acceleration so that the linear

interpolation is essentially perfect. If the time space  $\Delta t$  is constant, the coefficients A, B,.....D' need to be computed only once.

The exact solution of the equation of motion required in this numerical procedure is feasible only for linear systems. It is conveniently developed for SDF systems, as shown above, but would be impractical for MDF systems unless their response is obtained as superposition of modal responses.

#### 4.5 Newmark's Method

In 1959, N.M. Newmark developed a family of time-stepping methods based on the following equations

$$\dot{u}_{i+1} = \dot{u}_i + [(1 - \gamma)\Delta t]\ddot{u} + (\gamma\Delta t)\ddot{u}_{i+1} \quad (4.28)$$

$$u_{i+1} = u_i + (\Delta t)\dot{u}_i + [(.5 - \beta)(\Delta t)^2]\ddot{u}_i + [\beta(\Delta t)^2]\ddot{u}_{i+1} \quad (4.29)$$

The parameters  $\beta$  and  $\gamma$  define the variation of acceleration over time step and determine the stability and accuracy characteristics of the method. Typical selection for  $\gamma$  is  $\frac{1}{2}$  and  $\frac{1}{6} \leq \beta \leq \frac{1}{6}$  is satisfactory from all points of view, including that of accuracy.

Summarizes the time-stepping solution using Newmark's method as it might be implemented on the computer is presented in Table 4.3

#### 4.6 Theoretical Back Ground of SeismoSignal software

SeismoSignal constitutes an easy and efficient way to process strong-motion data, featuring a user-friendly visual interface and the capability of deriving a number of strong-motion parameters often required by engineer seismologists and earthquake engineers, such as:

- ❖ Fourier and Power spectra
- ❖ Elastic response spectra and pseudo spectra
- ❖ Over damped and constant-ductility inelastic response spectra
- ❖ Arias (Ia) and characteristic (Ic) intensities
- ❖ Cumulative absolute velocity (CAV) and specific energy density (SED)
- ❖ Root-mean-square (RMS) of acceleration, velocity and displacement
- ❖ Sustained maximum acceleration (SMA) and velocity (SMV)
- ❖ Effective design acceleration (EDA)
- ❖ Acceleration (ASI) and velocity (VSI) spectrum intensity

- ❖ Predominant ( $T_p$ ) and mean ( $T_m$ ) periods
- ❖ Husid and energy flux plots
- ❖ Bracketed, uniform, significant and effective durations

The program is able to read accelerograms defined in both single- and multiple-values per line formats (the two most popular formats used by strong-motion databases), which may then be filtered and baseline-corrected. Polynomials of up to the 3rd order may be employed for the latter, whilst three different digital filter types are available, all of which capable of carrying out high pass, low pass, band pass and band stop filtering.

Finally, and due to its full integration with the Windows environment, SeismoSignal allows for numerical and graphical results to be copied to any Windows application (e.g. MS Excel, MS Word, etc.), noting that the characteristics plots can be fully customised from within the program itself.

#### **4.7 Numerical Study**

In reference with the hazard curve and response spectrum obtained in chapter 3, seismic input parameters, especially artificial time - history is simulated. After determination of Single envelope function of Spectral Acceleration, duration and envelope function is determined using equation (4.12 to 4.19). Acceleration time history is generated using equation (4.1 to 4.11). Equation 4.4 represents the motion of single degree of freedom system, which is solved by using Method Based on Point of Interpolation of Excitation. Design earthquakes are simulated for calculated duration presented in Table 4.1. On the basis of above description a program is developed in Visual Fortran, which generates Time-Histories from given response spectrum. The generated time histories for bed rock and surface cases are presented in Fig.4.3 and Fig.4.4 respectively.

#### **4.8 Result and Discussion**

Target Spectrum as shown in Fig.4.5 is used for bed rock. The frequencies range considered is between .333 Hz to 50 Hz. The envelope curve is as shown in Fig.4.2. The 18.5,30 and 45 sec time-histories of the final iteration is shown in Fig. 4.3. Excellent convergence is achieved within twenty iterations, by considering 264 frequencies using equation (4.8).The calculated response spectrum envelopes the target spectrum closely at any frequency between .333 Hz to 50Hz. This spectrum closely matches the target spectrum as shown in Fig.4.5. From Fig.4.3, The maximum acceleration for 18.5 sec duration is 0.169 at time 4.5 sec and maximum acceleration for 30 sec duration is at time 9.84 sec.

Target Spectrum as shown in Fig.4.6 is used for Surface. The frequencies range considered is between .25Hz to 50 Hz. The envelope curve is as shown in Fig.4.2. The 20, 30 and 45 sec time-histories of the final iteration is shown in Fig. 4.4. Excellent convergence is achieved within twenty iterations, by considering 278 frequencies using equation (4.8).The calculated response spectrum envelopes the target spectrum closely at any frequency between .25 Hz to 50Hz. This spectrum closely matches the target spectrum as shown in Fig.4.6. From Fig.4.3, The maximum acceleration for 20 sec duration is 0.285 at time 2.94 sec and maximum acceleration for 30 sec duration is at time 9.88 sec.

The generated time- history for 18 sec as shown in Fig. 4.3 used in SeismoSignal and generated Spectrum (by SeismoSignal) is compare with the generated SA by a program developed in this research work is very closely matches each other as shown in Fig.4.7.

**Table 4.1 Weightage average duration for Center of Kathmandu City.**

Description	Durations		
	TD	TB	TC
For Rock	18.50	2.25	9.25
For Soil	20.00	2.50	10.00

**Table 4.2 COEFFICIENT IN RECURRENCE FORMULAS ( $\zeta < 1$ )**

$$A = e^{-\zeta\omega_n \Delta t} \left( \frac{\zeta}{\sqrt{1-\zeta^2}} \sin \omega_D \Delta t + \cos \omega_D \Delta t \right)$$

$$B = e^{-\zeta\omega_n \Delta t} \left( \frac{1}{\omega_D} \sin \omega_D \Delta t \right)$$

$$C = \frac{1}{K} \left\{ \frac{2\zeta}{\omega_n \Delta t} + e^{-\zeta\omega_n \Delta t} \left[ \left( \frac{1-2\zeta^2}{\omega_D \Delta t} - \frac{\zeta}{\sqrt{1-\zeta^2}} \right) \sin \omega_D \Delta t - \left( 1 + \frac{2\zeta}{\omega_n \Delta t} \right) \cos \omega_D \Delta t \right] \right\}$$

$$D = \frac{1}{K} \left\{ 1 - \frac{2\zeta}{\omega_n \Delta t} + e^{-\zeta\omega_n \Delta t} \left[ \left( \frac{2\zeta^2-1}{\omega_D \Delta t} \right) \sin \omega_D \Delta t - \left( \frac{2\zeta}{\omega_n \Delta t} \right) \cos \omega_D \Delta t \right] \right\}$$

$$A' = -e^{-\zeta\omega_n \Delta t} \left( \frac{\omega_n}{\sqrt{1-\zeta^2}} \sin \omega_D \Delta t \right)$$

$$B' = e^{-\zeta\omega_n \Delta t} \left( \frac{1}{\omega_D} \cos \omega_D \Delta t - \frac{\zeta}{\sqrt{1-\zeta^2}} \sin \omega_D \Delta t \right)$$

$$C' = \frac{1}{K} \left\{ \frac{1}{\Delta t} + e^{-\zeta\omega_n \Delta t} \left[ \left( \frac{\omega_n}{\sqrt{1-\zeta^2}} - \frac{\zeta}{\Delta t \sqrt{1-\zeta^2}} \right) \sin \omega_D \Delta t + \frac{1}{\Delta t} \cos \omega_D \Delta t \right] \right\}$$

$$D' = \frac{1}{K\Delta t} \left[ 1 - e^{-\zeta\omega_n \Delta t} \left( \frac{\zeta}{\sqrt{1-\zeta^2}} \sin \omega_D \Delta t + \cos \omega_D \Delta t \right) \right]$$



**Table 4.3 NEWMARK'S METHOD: LINEAR SYSTEMS**

Special Cases

(1) Average acceleration method  $\left(\gamma = \frac{1}{2}, \beta = \frac{1}{4}\right)$

(2) Linear acceleration method  $\left(\gamma = \frac{1}{2}, \beta = \frac{1}{6}\right)$

1. Initial Calculations

$$1.1 \ddot{u}_0 = \frac{p_0 - cu_0 - ku_0}{m}$$

1.2 Select  $\Delta t$ .

$$1.3 \hat{k} = k + \frac{\gamma}{\beta \Delta t} c + \frac{1}{\beta (\Delta t)^2} m$$

$$1.4 a = \frac{1}{\beta \Delta t} m + \frac{\gamma}{\beta} c; \text{ and } b = \frac{1}{2\beta} m + \Delta t \left(\frac{\gamma}{2\beta} - 1\right) c.$$

2. Calculation for each time step,  $i$

$$2.1 \Delta \hat{p}_i = \Delta p_i + a \dot{u}_i + b \ddot{u}_i$$

$$2.2 \Delta u_i = \frac{\Delta \hat{p}_i}{\hat{k}}$$

$$2.3 \Delta \dot{u}_i = \frac{\gamma}{\beta \Delta t} \Delta u_i - \frac{\gamma}{\beta} \dot{u}_i + \Delta t \left(1 - \frac{\gamma}{2\beta}\right) \ddot{u}_i$$

$$2.4 \Delta \ddot{u}_i = \frac{1}{\beta (\Delta t)^2} \Delta u_i - \frac{1}{\beta \Delta t} \dot{u}_i - \frac{1}{2\beta} \ddot{u}_i$$

$$2.5 u_{i+1} = u_i + \Delta u_i, \dot{u}_{i+1} = \dot{u}_i + \Delta \dot{u}_i$$

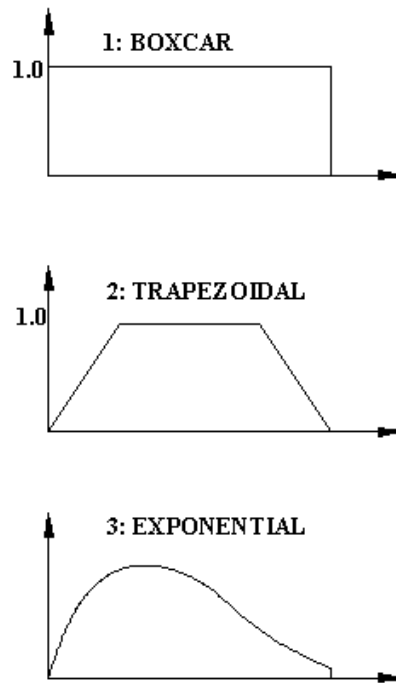


Fig. 4.1 Intensity envelope function  $F(t)$

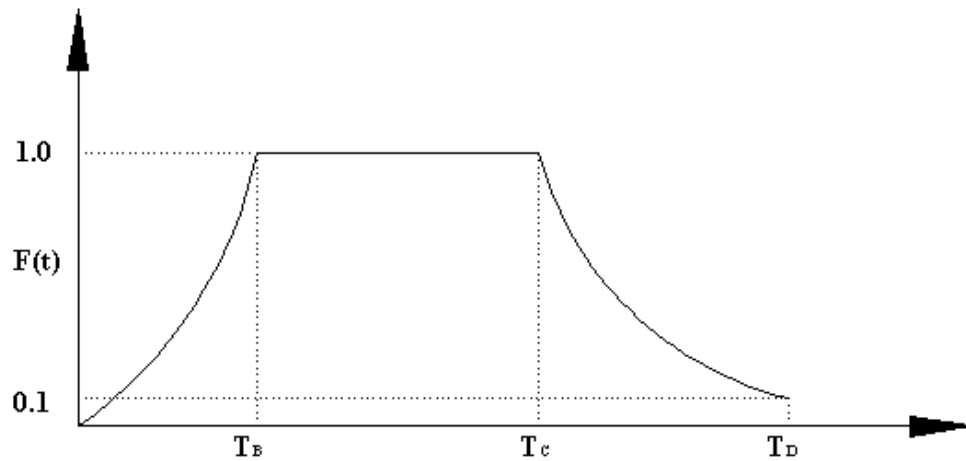
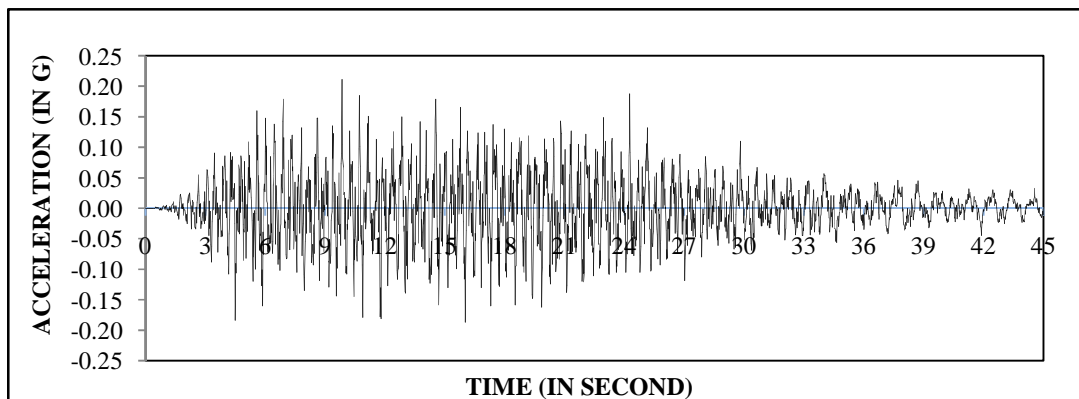
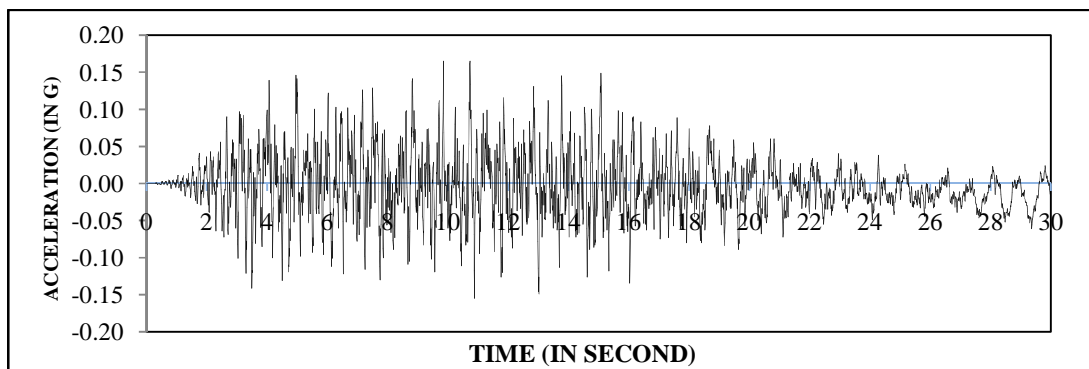
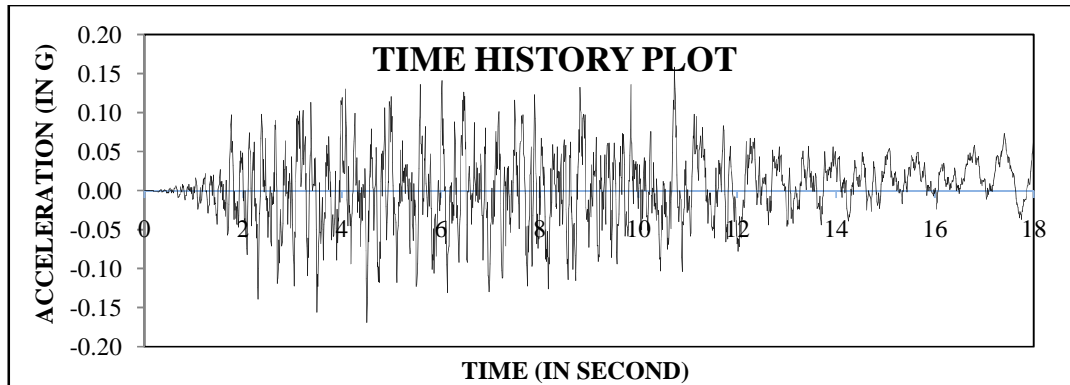
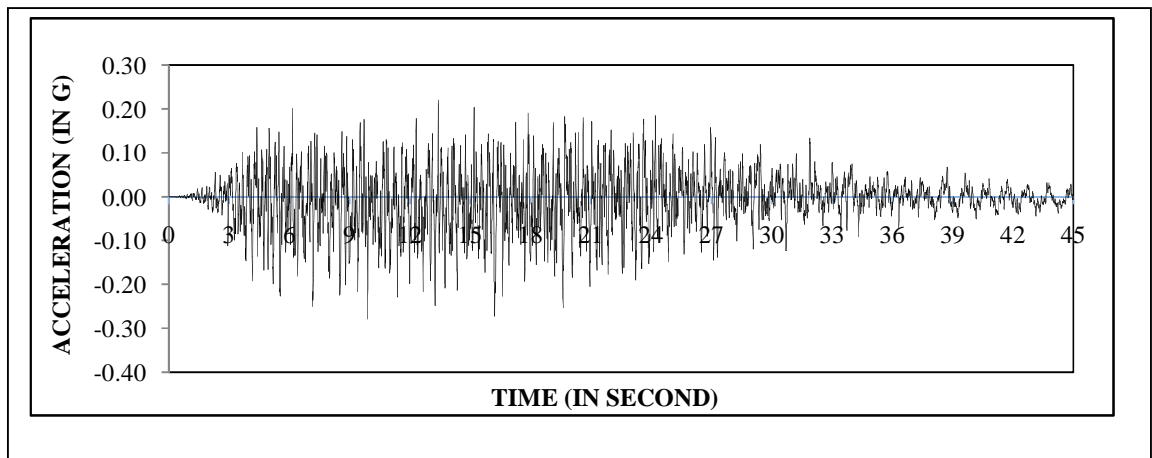
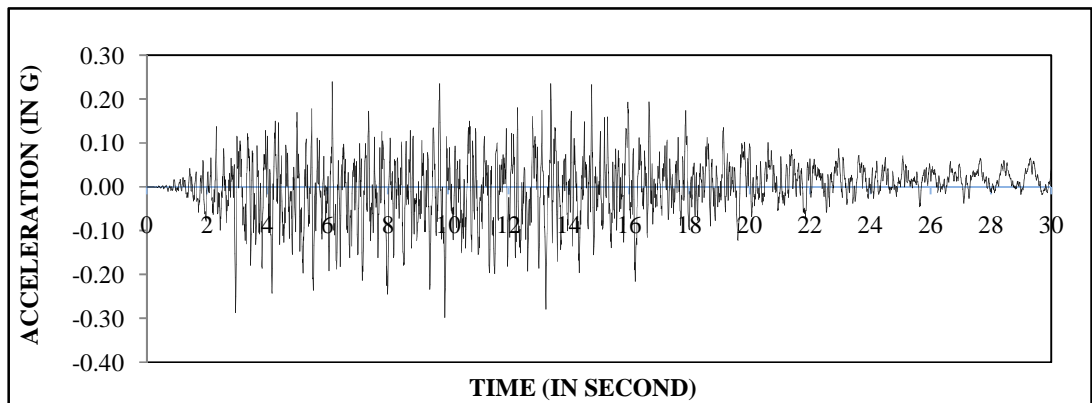
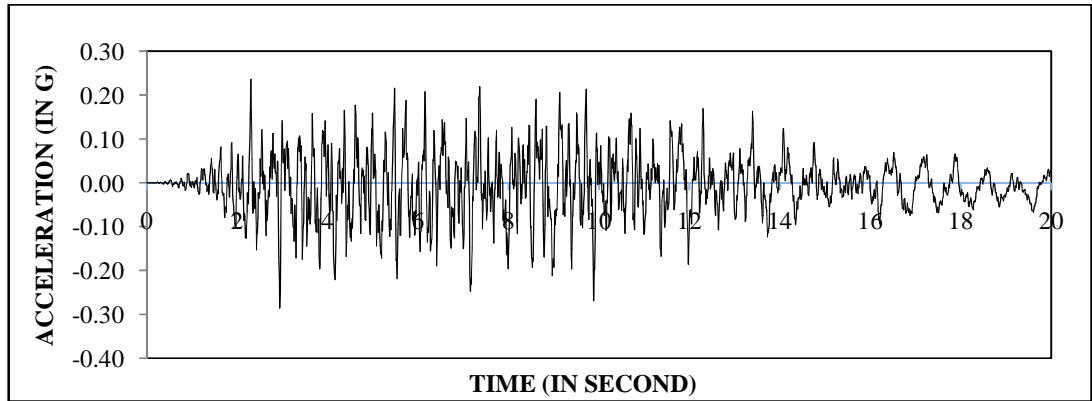


Fig. 4.2 Division of duration and envelope function.



**Fig. 4.3 Simulated Time histories for Center of Kathmandu City at bed rock level.**



**Fig. 4.4 Simulated Time - Histories for Center of Kathmandu City.**

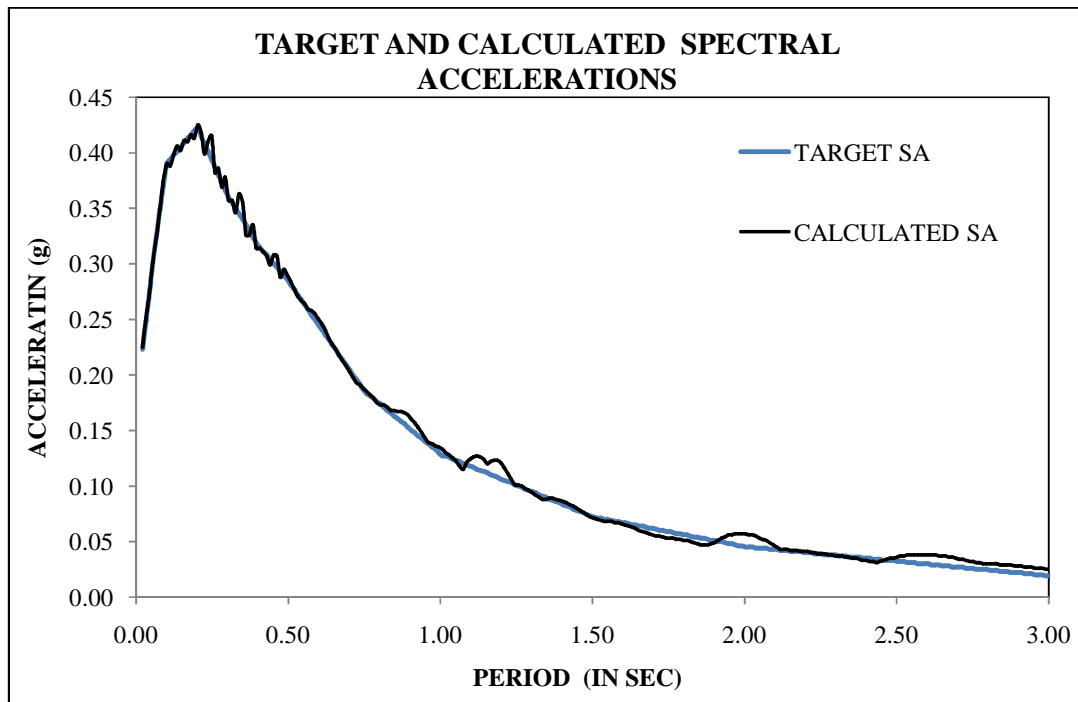


**Fig. 4.5 Spectral Acceleration for Center of Kathmandu at bed rock level.**

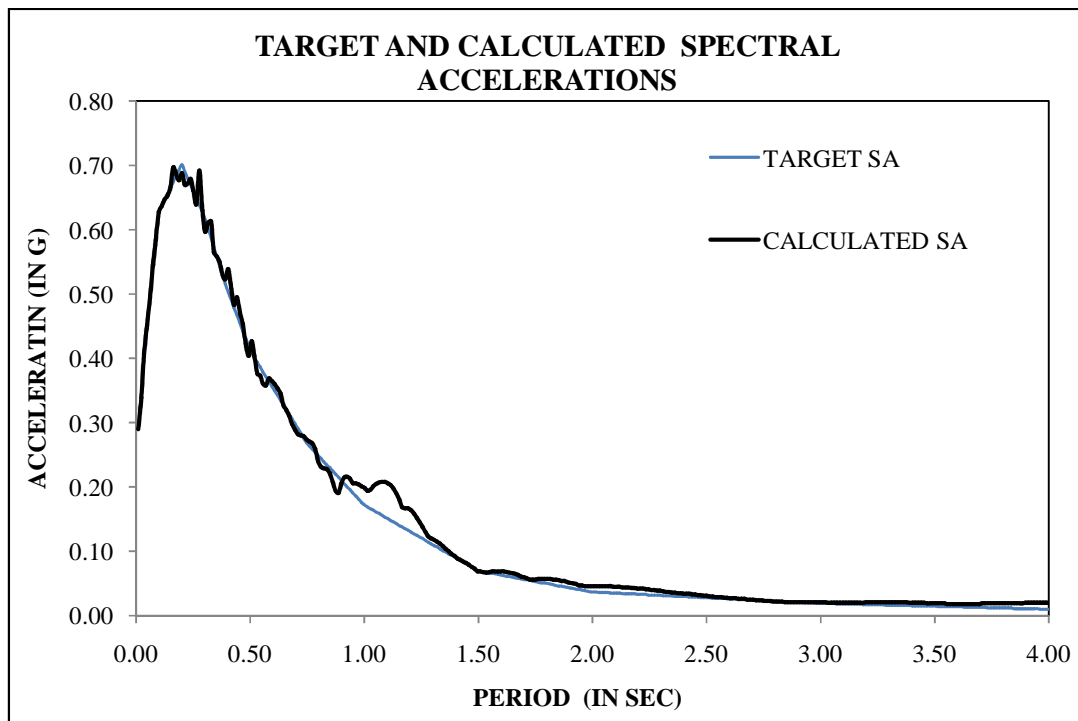


**Fig. 4.6 Spectral Acceleration for Center of Kathmandu at Surface level.**

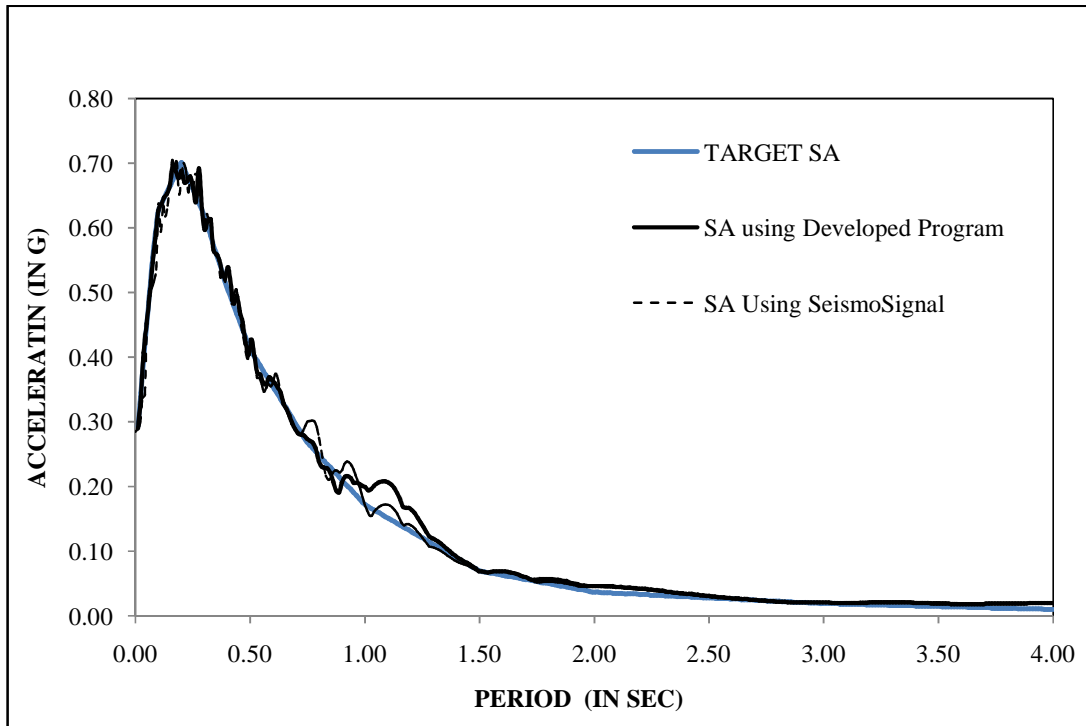


**Fig. 4.7 Comparison of Spectral Acceleration using SeismoSignal Software and developed Program.**

## Appendix 4A: (Program Coding)

```

C      *****
C      **THIS IS PROGRAM TO GENERATE TIME HISTORY FROM GIVEN RESPONSE
SPECTRA*****
C      **DEVELOPED BY ER. SHAILENDRA KUMAR SAH, UDER THE SUPERVISION OF
PROF. DR. P.N. MASKEY*****
C      *****

DIMENSION FR(5000),VMAX(5000),V(5000,150),FF(5000),T(5000)
DIMENSION A(5000,150),W(5000,150),WD(5000,150),E(5000,150)
DIMENSION F(5000,150),G(5000,150),AA(5000,150),B(5000,150)
DIMENSION Q(5000,150),QQ(5000,150),C(5000,150),R(5000,150)
DIMENSION RR(5000,150),D(5000,150),AAA(5000,150),BB(5000,150)
DIMENSION CC(5000,150),DD(5000,150),UD(5000,150),UV(5000,150)
DIMENSION UA(5000,150),SC(5000,150),SA(5000,150),TF(5000)
DIMENSION S(5000,150),H(5000,150),HH(1500),UAA(5000,150)
DIMENSION HHH (5000), HHHH (5000), HHC1 (5000, 150), HHC2 (5000, 150)
REAL TI, TD, TB, TC

C      **DESCRIPTION OF SYMBOL*****
C      N=NUMBER OF DATA FOR TARGET SPECTRAL ORDINATE
C      TD=TI "TOTAL DURATION OF EARTH QUAKE"
C      TB=IN THE FIRST PART UP TO TB ACCELERATION WILL BE ASSENDING
C      TC=IT IS MUCH EFFECTIVE
C      Z=ZIE

C      **READ INPUT DATA i.e. PERIOD & TARGET SPECTRAL ACCELEARATION*****
WRITE (*,*)'ENTER THE NO OF DATA TO BE READ, ZIE AND TIME PERIOD'
READ (*,*) N, Z, TI
OPEN (1, FILE='SEISM.TXT', STATUS='OLD')
DO 100 I=1, N
100 READ (1,*) TF (I), SA (I, 1)
NN=TI/.01
PI=3.1415927
TD=TI
TB=TD*.10
TC=TD*.50

C      **GENERATION OF ENVELOPE FUNCTION*****

```

```

X=1
DO 1500 KC=1, N
1500 A (KC, X) =1.5*Z*SA (KC, 1)
888 ZZZZZ=0
DO 200 J=1, NN
T (J) = (J-1)*TI/(NN-1)
IF (T (J).LE.TB) GO TO 123
IF (T (J).LE.TC) GO TO 223
FF (J) =EXP (-2.3025*(T (J)-TC)/ (TD-TC))
GO TO 423
223 FF (J) =1.0
GO TO 423
123 FF (J) = (T (J)/TB) **2

C *****GENERATION OF ACCELERATION*****
423 HH (J) =0
DO 300 K=1, N
FR (K) =1.0/TF (K)
HH (K) =HH (J)
HHH (K) =HHH (J)
HH(J)=(-1)**K*A(K,X)*SIN(2*PI*FR(K)*T(J))+HH(K)
HHH(J)=-(-1)**K*A(K,X)*(COS(2*PI*FR(K)*T(J))-1)/(2*PI*FR(K))+
CHHH (K)
HHHH(J)=-(-1)**K*A(K,X)*(SIN(2*PI*FR(K)*T(J))/(2*PI*FR(K))-
CT (J))/ (2*PI*FR (K)) +HHHH (K)
300 CONTINUE
H (J, X) =FF (J)*HH (J)*9.81
HHC1 (J, X) =FF (J)*HHH (J)*9.81
HHC2 (J, X) =FF (J)*HHHH (J)*9.81
200 CONTINUE

C **CORRECTION OF THE GROUND ACCELERATION TIME HISORY*****
CC1=HHC1 (NN, X)
CC2=HHC2 (NN, X)
AA1=6*(CC1*TI-4*CC2)/ (TI**3)
BB1=12*(3*CC2-CC1 *TI)/ (TI**4)
DO 1100 IZ=1, NN
1100 H(IZ,X)=(H(IZ,X)+AA1 *T(IZ)+BB1 *T(IZ)*T(IZ))

C **CHEC FOR ITERATION *****

```



```

ITERATION=X
IF (ITERATION.EQ.20) GO TO 999

C   **DETERMINATION OF SPECTRAL ORDINATE FROM GENERATED
ACCELERATION TIME HISTORY*****
C   **USING METHOD BASED ON INTERPOLATION OF EXCITATION*****
DO 400 L=1, N
W (L, X) =2*PI*FR (L)
WD (L, X) =W (L, X)*SQRT (1-Z*Z)
DT=TI/NN
E (L, X) =EXP (-Z*W (L, X)*DT)
S (L, X) =SIN (WD (L, X)*DT)
F (L, X) =COS (WD (L, X)*DT)
G (L, X) =Z/SQRT (1-Z*Z)
AA(L,X)=E(L,X)*(G(L,X)*S(L,X)+F(L,X))
B (L, X) =E (L, X)*(1/WD (L, X)*S (L,X))
C(L,X)=1/(W(L,X)*W(L,X))*(2*Z/(W(L,X)*DT)+E(L,X)*(((1-2*Z*Z)/(WD(L,X)*DT)-
G(L,X))*S(L,X)-(1+2*Z/(W(L,X)*DT))*F(L,X)))
D(L,X)=1/(W(L,X)*W(L,X))*(1-2*Z/(W(L,X)*DT)+E(L,X)*((2*Z*Z-1)/
(WD(L,X)*DT)*S(L,X)+2*Z/(W(L,X)*DT)*F(L,X)))
AAA(L,X)=-E(L,X)*(W(L,X)/SQRT(1-Z*Z)*S(L,X))
BB(L,X)=E(L,X)*(F(L,X)-G(L,X)*S(L,X))
CC(L,X)=1/(W(L,X)*W(L,X))*(-1/DT+E(L,X)*((W(L,X)/SQRT(1-Z*Z)
+G(L,X)/DT)*S(L,X)+1/DT*F(L,X)))
DD(L,X)=1/(W(L,X)*W(L,X)*DT)*(1-E(L,X)*(G(L,X)*S(L,X)+F(L,X)))
UD (1, X) =0.0
UV (1, X) =0.0
UA (1, X) =0.0
UDMAX=0.0
UVMAX=0.0
UAMAX=0.0

C   *****DETERMINATION OF MAXIMUM DISPLACEMENT*****
NN1=NN-1
DO 500 M=1, NN1
UD(M+1,X)=AA(L,X)*UD(M,X)+B(L,X)*UV(M,X)+C(L,X)*H(M,X)+D(L,X)*H(M+1,X)
UV(M+1,X)=AAA(L,X)*UD(M,X)+BB(L,X)*UV(M,X)+CC(L,X)*H(M,X)+DD(L,X)*H(M
+1,X)
UA(M+1,X)=-W(L,X)*W(L,X)*UD(M+1,X)-2*Z*W(L,X)*UV(M+1,X)+H(M+1,X)
IF (ABS (UDMAX).LT.ABS (UD (M, X))) UDMAX=UD (M, X)

```

```

500 CONTINUE

C    **DETERMINATION OF MAXIMUM RESPONSE SA FOR EACH FREQUENCY*****
SC (L, X) = (W (L, X)*W (L, X))*ABS (UDMAX)/9.81
V (L, X) =ABS (SA (L, 1)/SC (L, X)-1)
400 CONTINUE
VMAX(X)=V(1,X)
DO 700 IV=2, N
IF (VMAX(X).LT.V (IV, X)) VMAX(X) =V (IV, X)
700 CONTINUE
IF (VMAX(X).LE..05) GO TO 999
X=X+1
DO 900 IY=1, N
900 A(IY,X)=(SA(IY,1)/SC(IY,X-1))*1.15*A(IY,X-1)
GO TO 888

C    **OUTPUT OF TARGET SPECTRAL ORDINATE & CALCULATED SPECTRAL ORDINATE***
999 XXX=0
OPEN (2, FILE='SPECTRL.XLS', STATUS='NEW')
DO 1300 JC=1, N
WRITE(2,10)TF(JC),SC(JC,X-1),SA(JC,1)
10  FORMAT (3F10.3)
1300 CONTINUE

C    **GENERATED ACCELERATION TIME HISTORY*****
OPEN (3, FILE='TIMEHISTORY.XLS', STATUS='NEW')
DO 1400 JT=1, NN
H (JT, X) =H (JT, X)/9.81
WRITE (3, 15) T (JT), H (JT, X)
15  FORMAT (2F10.3)
1400 CONTINUE
ENDFILE 3
ENDFILE 2
ENDFILE 1
STOP
END

```

## 5. CONCLUSION AND RECOMMENDATIONS

### 5.1 General Conclusion

The probabilistic seismic hazard analysis is carried out for the Center of Kathmandu region which is surrounded by 10-active faults. It is assumed that the probabilistic distribution in time is poisson's distribution, and within the source zone, epicenters are uniformly spatially distributed. Various attenuation laws are studied out of which one attenuation law given by Young's et al (1997) to be considered to obtain the Hazard curves at the site. Time history at the bed rock of Center of Kathmandu city is obtain by developing a program in Visual Fortran using a technique given by M.R. Khan. The program developed to be used to generate time history of site from given response spectrum.

### 5.2 Major Conclusion

From the results of the study, the following major conclusions are drawn:

- 1) The seismic hazard curve at the bedrock and free field obtained by using attenuation law given by young's et al (1997). The PGA values having 10% probability of exceedence obtained is .32g for bed rock and .39g for free field.
- 2) The study shows that the contribution of Source Gosai-Kunda (MCT-3.3) in Seismic Hazard Analysis is larger in compare to other sources and it is considered to be the vulnerable source for Kathmandu City.
- 3) Spectral Acceleration correspond to the different structural time period are obtain for bed rock as well as free field.
- 4) Single envelope of Spectral Acceleration for both bed rock and free field are determined separately. Peak of SA in case of bed rock is .42g at period .2 sec and Peak of SA in case of free field is .70g at period .2 sec.
- 5) The program developed in Visual Fortran gives the good result within the 20 iterations.
- 6) The generated time-history used in SeismoSignal and Spectrum generated (by SeismoSignal) is compare with the program developed in this research work is very closely matches each other.
- 7) The purposed method described in this thesis work converges rapidly and

very closely to the target spectra and generated time histories rich in all frequencies.

### **5.3 Recommendations**

Here recommendation is made for the recently developed Program to be used for the generation of Ground motion parameter for Nepal region for engineering purpose.

The study may be extended by considering various conditions and parameters. It is recommended that the research in the following areas be further

- Simulation of Time history considering soil amplification effect on the surface of site.
- Seismic Microzonation of Kathmandu region
- Reliability Analysis of structures in Kathmandu Region.
- Simulation of Time history considering Different type Envelope to be considered.

## REFERENCES

1. **Youngs R.R., Chiou S.J., Silva W.J. and Humphrey J.R. (1997)** “*Strong motion attenuation relationships for subduction zone earthquakes,*” Seismological research letters Vol. 68, No -1, pp. 58-73.
2. **Khan M.R., (1987)** “*Improved method of generation of artificial time histories, rich in all frequencies, from floor spectra*” Earthquake engineering and structural dynamics Vol. 15 pp. 985-992.
3. **Chopra A.K. (2003).** *Dynamics of structures: Theory and applications to earthquake engineering*, Pearson education.
4. **Clough R.W. and Penzienj.** *Dynamics of Structures, 2<sup>nd</sup> edition*, McGraw-Hill.
5. **Kramer S.L.(2003).** *Geotechnical earthquake Engineering*, Prentice-Hall International Series in Civil Engineering and Engineering mechanics, William J. Hall, Editor.
6. **Paz M. (1997).** *Structural dynamics: Theory and computation*, Chapman and Hall.
7. **Yang C. Y. (1986).** *Random vibration of Structures*. A Wiley-Interscience publication.
8. **Pandey M.R., Chitrakar G.R., Kafle B., Sapkota S.N., Rajpune S., Gautam U.P. (2002).** *Seismic hazard map of Nepal*.
9. **Maskey P.N. and Mishra H.K. (2005)** “*Selection of attenuation laws for estimation of seismic input in Nepal,*” Journal of the Institute of Engineering, Vol. 5 No.1, pp.75-85.
10. **Maskey P.N. (2003)** “*Seismic Microzonation of a Typical region of Kathmandu valley*” Journal of the Institute of engineering Vol. 3, No.1, pp. 1-11.
11. **Matheu E.E., Yule D.E. and Kala R.V. (2005)** “*Determination of standard response spectra and effective peak ground acceleration for seismic design and evaluation*” ERDC/CHL CHETN- Vol-41, pp.1-16.
12. **Paul Lai S.S. (1982)** “*Statical Characterization of strong ground motion using power spectral density functions,*” Bulletin of the Seismological society of America, Vol-72, No.1, PP. 259-274.

13. **Adnan A., Hendriyawan, Marto A. and Irsyam M. (2006)** “*Development of synthetic time histories at bed rock for Kualalumpur,*” Proceeding and Construction conference (APSEC2006) Kualalumpur, Malaysia PP. E- 34 to E47.
14. **Xavier C. (2000).** *Fortran77 and Numerical method.*
15. **Iyengar R.N. and Rao P.N. (1979)** “*Generation of Spectrum Compatible Accelerograms,*” Earthquake Engineering and Structural Dynamics, Vol.7, pp. 253-263.
16. **Wogn H.L. and Trifunac M.D. (1979)** “*Generation of Artificial strong motion accelerograms,*” Earthquake Engineering and Structural dynamics Vol.7, pp.509-527.
17. **Idriss, I.M. and Archuleta R.J.(2007)** “*Evaluation of Earthquake ground motion,*” Division of Dam safety and Inspection office of Hydropower Licensing federal Energy Regulatory Commission. Washington, D.C. Dreyt065
18. **Jennings P.C., Housner G.W. and Tsai N.C. (1968)** “*Simulated Earthquake Motions,*” A report on research conducted under a grant from the national Science Foundation Pasadena, California.
19. **Sharma R.D., Gupta S. and Kumar S. (1999)** “*Application of Extreme-value Distribution for Estimating Earthquake Magnitude- Frequency relationships,*” ISET Journal of Earthquake Technology paper No. 388, Vol. 36, No.1, pp. 15-26.
20. **Wang J, Fan L., Qian Sand Zhou J. (2002)**”*Simulations of non- stationary frequency content and its importance to seismic assessment of structures,*” Earthquake Engineering and Structural Dynamics Vol. 31, pp. 993-1005.
21. **Yuen K.V., Beck G.L. and Katafygiotis L.S. (2002)** “*Probabilistic approach for modal identification using non-stationary noisy response measurements only,*” Earthquake Engineering and Structural Dynamics Vol31, pp1007-1023.
22. **Takada T., Okumura T., Hirose J., Muramatsu K., Taki S. and Ishii K.** “*Probabilistic Scenario Earthquakes for Seismic Design - Comparism of two Identification Procedures,*” Reactor safety analysis lab, JAERI, Ohasaki Research Institute, University of Tokyo.

23. **Takada T. and Ochi S. (2004)** “*Probability based Determination of Design Earthquakes,*” IFED International Forum on Engineering Decision making, Switzerland.
24. **Jian-wen S. and Shu-Zhong S. (2004)** “*Probability- Consistent Spectrum and Code spectrum*” ACTA Seismologica Sinica, Vol. 17, No. 1 pp. 99-108.
25. **Okawa I., Kashima T., Kitamura H., Tohdo M., Sakai S., Tanigalci M., Yamagishi K. and Nariika K.** “*On the Generation of the design earthquake ground motion time history*”.
26. **Atkinson G.M. and Boone D.M. (2003)** “*Empirical Ground Motion Relations for Subduction Zone Earthquake and their applications to Casacadia and other regions,*” Bulletin of the seismological Society of America, Vol. 93, No. 4. Pp. 1703-1729.
27. **Signh V.N. and Mittal A. (2005)** “*Synthetic Accelerograms for two Himalayan Earthquakes using Convolution,*” Current Science, Vol. 88, No. 8, pp. 1289-1297.
28. **T.G. Sitaram, P. Anbazhangan and K. Ganesh Raj (2006)** “*Use of remote sensing and seismotectonic parameters for seismic hazard analysis of Bangalore,*” Natural Hazard and Earth system Science Vol. 6, pp. 927-939.
29. **Iyengar R.N. (1993)** “*Spectrum Compatible Nonstationary Earthquake modal,*” Department of Civil Engineering Indian Institute of Science Bangalore.
30. **Weiner E. O.** “*Design spectra Development considering short time history,*” Plant Analysis, Westinghouse Hanford Company, Richland.
31. **Kimura M. and Izumi M. (1989)** “*A Method of Artificial Generation of Earthquake Ground Motion,*” Earthquake Engineering and Structural Dynamics, Vol. 18, pp. 867-874.
32. **Prajuli H., Kiyono J., ONO Yusuke and Tsutsumiuchi T. (2008)** “*Design Earthquake Ground Motion from Probabilistic Response Spectra Case study of Nepal,*” Journal of Japan Association for Earthquake Engineering, Vol.8, No.4.
33. **Safak E. (1988)** “*Analytical Approach to Calculate Response Spectra from Seismological Models of Ground Motion,*” Earthquake Engineering and Structural Dynamics, Vol. 16, pp. 121-134.

34. **Crespi G.P. Floris C. and Paganine P. (2000)** “*A Probabilistic Method for Generating Spectrum Compatible earthquake time histories,*” European Earthquake Engineering, 3, 2000.
35. Shah Y. (2003) “*Probabilistic Seismic Input for Pokhara Region of Nepal,*” Thesis No: S0071, TU, IOE, Pulchowk Campus.
36. Mishra S.K. (2004) “*Attenuation of Ground Motion for the Region,*” Thesis No: S0075, TU, IOE, Pulchowk Campus



## **Appendix:-**

## APPENDIX A

### ATTENUATION RELATIONSHIPS FOR SUBDUCTION EARTHQUAKES

The attenuation relationships derived by Youngs et al (1997) is summarized in this Appendix.

The following attenuation relationship was derived by Youngs et al (1997):

Attenuation Relationships for Horizontal Response Spectral Acceleration (5% Damping) for Subduction Earthquakes.

**For Rock.**

$$\ln(\text{PGA}) = .2418 + 1.414M - C_1 + C_2(10-M)^3 + C_3 \ln(r_{rup} + 1.7818e^{-554M}) + .00607H$$

$$\text{Standard Deviation} = C_4 + C_5M$$

The values of the coefficient  $C_1, \dots, C_5$  are listed in Table A-1

Table A-1 Coefficients of Attenuation Equations Derived by Young et al (1997)

Period - Sec	C1	C2	C3	C4	C5
PGA	0.000	0.0000	-2.552	1.45	-0.10
0.075	1.275	0.0000	-2.707	1.45	-0.10
0.100	1.188	-0.0011	-2.655	1.45	-0.10
0.200	0.722	-0.0027	-2.528	1.45	-0.10
0.300	0.246	-0.0036	-2.454	1.45	-0.10
0.400	-0.115	-0.0043	-2.401	1.45	-0.10
0.500	-0.400	-0.0048	-2.360	1.45	-0.10
0.750	-1.149	-0.0057	-2.286	1.45	-0.10
1.000	-1.736	-0.0064	-2.234	1.45	-0.10
1.500	-2.634	-0.0073	-2.160	1.50	-0.10
2.000	-3.328	-0.0080	-2.107	1.55	-0.10
3.000	-4.511	-0.0089	-2.033	1.65	-0.10

**For Soil**

$$\ln(\text{PGA}) = -0.6687 + 1.438M - C_1 + C_2(10-M)^3 + C_3 \ln(r_{\text{rup}} + 1.097e^{-0.617M}) + 0.00648H$$

$$\text{Standard Deviation} = C_4 + C_5M$$

The values of the coefficient  $C_1, \dots, C_5$  are listed in Table A-2

Table A-2 Coefficients of Attenuation Equations Derived by Young et al (1997)

Period - Sec	C1	C2	C3	C4	C5
PGA	0.000	0.0000	-2.329	1.45	-0.10
0.075	2.400	-0.0019	-2.697	1.45	-0.10
0.100	2.516	-0.0019	-2.697	1.45	-0.10
0.200	1.549	-0.0019	-2.464	1.45	-0.10
0.300	0.793	-0.0020	-2.327	1.45	-0.10
0.400	0.144	-0.0020	-2.230	1.45	-0.10
0.500	-0.438	-0.0035	-2.140	1.45	-0.10
0.750	-1.704	-0.0048	-1.952	1.45	-0.10
1.000	-2.870	-0.0066	-1.785	1.45	-0.10
1.500	-5.101	-0.0114	-1.470	1.50	-0.10
2.000	-6.433	-0.0164	-1.290	1.55	-0.10
3.000	-6.672	-0.0221	-1.347	1.65	-0.10
4.000	-7.618	-0.0235	-1.272	1.65	-0.10

$r_{\text{rup}}$  = Closest distance to rupture (Km)

M = moment magnitude

H = depth (Km)

Standard Deviation for magnitudes greater than M8 set equal to the value for M8

## Appendix: B-1

### Response Spectral Acceleration (5% damping) for Rock

0.010	0.198
0.075	0.344
0.100	0.390
0.200	0.423
0.300	0.362
0.400	0.317
0.500	0.285
0.750	0.185
1.000	0.129
1.500	0.072
2.000	0.045
3.000	0.019

### Response Spectral Acceleration (5% damping) for Soil

0.010	0.293
0.075	0.560
0.100	0.629
0.200	0.702
0.300	0.619
0.400	0.506
0.500	0.412
0.750	0.267
1.000	0.172
1.500	0.070
2.000	0.037
3.000	0.019
4.000	0.010